Research

Molecular Consequences of Proprotein Convertase 1/3 (PC1/3) Inhibition in Macrophages for Application to Cancer Immunotherapy: A Proteomic Study*[S]

Marie Duhamel‡, Franck Rodet‡, Nadira Delhem§, Fabien Vanden Abeele¶, Firas Kobeissy‖, Serge Nataf, Laurent Pays**, Roxanne Desjardins‡‡, Hugo Gagnon§§, Maxence Wisztorski‡, Isabelle Fournier‡, Robert Day‡‡, and Michel Salzet‡¶¶**

Macrophages provide the first line of host immune defense. Their activation triggers the secretion of pro-inflammatory cytokines and chemokines recruiting other immune cells. In cancer, macrophages present an M2 anti-inflammatory phenotype promoting tumor growth. In this way, strategies need to be develop to reactivate macrophages. Previously thought to be expressed only in cells with a neural/neuroendocrine phenotype, the proprotein convertase 1/3 has been shown to also be expressed in macrophages and regulated as a function of the Toll-like receptor immune response. Here, we investigated the intracellular impact of the down-regulation of the proprotein convertase 1/3 in NR8383 macrophages and confirmed the results on macrophages from PC1/3 deficient mice. A complete proteomic study of secretomes and intracellular proteins was undertaken and revealed that inhibition of proprotein convertase 1/3 orient macrophages toward an M1 activated phenotype. This phenotype is characterized by filopodial extensions, Toll-like receptor 4 MyD88-dependent signaling, calcium entry augmentation and the secretion of pro-inflammatory factors. In response to endotoxin/lipopolysaccharide, these intracellular modifications increased, and the secreted factors attracted naïve T helper lymphocytes to promote the cytotoxic response. Importantly, the application of these factors onto breast and ovarian cancer cells resulted in a decrease viability or resistance. Under inhibitory conditions using interleukin 10, PC1/3-knockdown macrophages continued to secrete inflammatory factors. These data indicate that targeted inhibition of proprotein convertase 1/3 could represent a novel type of immune therapy to reactivate intra-tumoral macrophages. ***Molecular & Cellular Proteomics 14: 10.1074/mcp.M115.052480, 2857–2877, 2015.***

From the ‡Inserm U-1192, Laboratoire de Protéomique, Réponse Inflammatoire, Spectrométrie de Masse (PRISM), Université Lille 1, Cité Scientifique, 59655 Villeneuve D'Ascq, France; §Institut de Biologie de Lille, UMR 8161 CNRS, Institut Pasteur de Lille, Université Lille 1, Lille, France; ¶Inserm U-1003, Equipe labellisée par la Ligue Nationale contre le cancer, Laboratory of Excellence, Ion Channels Science and Therapeutics, Université Lille 1, Cité Scientifique, 59655 Villeneuve d'Ascq, France; ‖Department of Biochemistry and Molecular Genetics, Faculty of Medicine, American University of Beirut; **Inserm U-1060, CarMeN Laboratory, Banque de Tissus et de Cellules des Hospices Civils de Lyon, Université Lyon-1; ‡‡Institut de Pharmacologie, Département de Chirurgie/Service d'Urologie, Faculté de Médecine et des Sciences de la Santé, Université de Sherbrooke, Sherbrooke, J1H 5N4 Québec, Canada; §§PhenoSwitch Bioscience Inc. 3001 12e Ave Nord, Sherbrooke, Qc, Canada, J1H 5N4

Received June 3, 2015, and in revised form, August 25, 2015
Published, MCP Papers in Press, September 1, 2015, DOI 10.1074/mcp.M115.052480
Author's contributions: MS, MD, RD wrote the paper. MD, FR, MW, FVA, ND, FK, HG, RoD performed the experiments. MS, IF, RD received financial support for the project and corrected the manuscript. All authors reviewed the manuscript.

Innate immunity is the first line of immune defense and is common to all metazoans (1, 2). In this immune system, macrophages play a crucial role in the maintenance of tissue homeostasis. These cells are involved in almost every disease through their immunological and wound-healing functions (1, 2). During a pathogenic infection, trauma or neurodegeneration, macrophages are recruited and activated contributing to the phagocytosis of pathogens and the secretion of cytokines and chemokines activating other immune cells. Macrophages can develop into classically pro-inflammatory (M1) or alternatively (M2) activated macrophages. M1 macrophages are characterized by the secretion of pro-inflammatory cytokines whereas M2 macrophages secrete anti-inflammatory cytokines (3). Stimulation of macrophages with LPS activates TLR4 signaling leading to the nucleus translocation of NF-κB or IRF3 which activate genes encoding proteins involved in innate immune response (4). Many of these proteins are secreted (cytokines, chemokines…) to attract and activate other immune cells like T lymphocytes. In tumors, macrophages are oriented toward the M2 phenotype and promote cancer growth by suppressing immune cells function (5). Current

research in the therapeutic field focus on ways to reactivate macrophages.

Surprisingly, we have shown that during immune responses, macrophages secrete typical neuroendocrine molecules (6–8), such as neuropeptides (9) or the proprotein convertases (PC)[1] PC2 and PC1/3 and that PC1/3 is an important regulator of innate immune responses (10–12). Proprotein convertases cleave precursor proteins which can lead to the activation, inactivation or functional changes. PC2 and PC1/3 operate within the regulated secretory pathway. Their expression is not restricted to neuroendocrine tissues, they are also expressed in macrophages and lymphocytes (12). In a previous study from our group, PC1/3 knockout (KO) in mice challenged with LPS caused innate immune defects and uncontrolled cytokine secretion (10). Th1 pathway is enhanced in PC1/3 KO mice. Following LPS treatment, PC1/3 colocalized with TLR4 in the endosomal compartment (11). We concluded that PC1/3 contributes to the regulation of TLR4 signaling and the resulting cytokine secretion.

The NR8383 rat pulmonary macrophage cell line was previously shown as a good model to study the role of PC1/3 in the macrophage innate immune response (13). In the present study, we developed a PC1/3-knockdown (K_D) NR8383 cell line using lentiviral-delivered shRNAs. Our aim is to understand the cellular impact of PC1/3 inhibition in macrophages and the consequences on their activation. Proteomic analysis of secreted proteins allowed us to identify pro-inflammatory cytokines and alarmins already at 24h of LPS stimulation in PC1/3-K_D secretomes which was confirmed by cytokines array. Proteomic studies of PC1/3-K_D NR8383 cellular extracts revealed an important perturbation in the intracellular trafficking machinery through the disorganization of cytoskeletal protein expression. These results were confirmed on macrophages from PC1/3 KO mice. Cytokines secretion and cytoskeleton reorganization can be linked to intracellular calcium increase in PC1/3-K_D cells. Moreover, we showed that MyD88-dependant TLR4 signaling was sustained when PC1/3 is down-regulated. We describe here that inhibition of PC1/3 induced classically activated phenotype (M1) in macrophages. The chemotactic and anti-tumor properties of the PC1/3-K_D macrophage secretome promoted the cytotoxic immune response and inhibited cancer cell viability. The down-regulation of PC1/3 could be used in cancer immunotherapy to reactivate macrophages.

[1] The abbreviations used are: PC, proprotein convertase; KO, knock-out; LPS, lipopolysaccharide; TLR, Toll-like receptor; KD, knock-down; SOC, Store-operated channel; NT, nontarget; PFA, paraformaldehyde; OVA, ovalbumine; FBS, fetal bovine serum; FASP, filter aided sample preparation; HCD, higher energy collision dissociation; FDR, false discovery rate; NK, natural killer; RLU, relative light unit; CCL, chemokine (C-C motif) ligand; CXCL, chemokine (C-X-C motif) ligand; MIF, macrophage migration inhibitory factor; WASP, Wiskott–Aldrich syndrome protein; TGN, trans-golgi network; ECV, endosome carrier vesicle; MVB, multivesicular body; TG, thapsigargin; ER, endoplasmic reticulum; SOCE, store-operated calcium entry; NA, nonactivated; A, activated; shRNA, small hairpin RNA; NaF, sodium fluoride; NP40, Nonidep P-40; LFQ, label free quantification; HBSS, Hank's balanced salt solution; PBMC, peripheral blood mononuclear cell.

EXPERIMENTAL PROCEDURES

Cell Culture—The rat alveolar macrophage cell line NR8383 (CRL-2192) was obtained from ATCC (Manassas, VA). NR8383 PC1/3-K_D and NR8383 nontarget (NT) shRNA cell lines were cultured in Ham's F12K medium supplemented with 15% fetal bovine serum and 12 μg/ml puromycin at 37 °C in a humidified atmosphere (5% CO_2). NR8383 PC1/3 K_D was performed using lentivirus transduction as described previously (11).

Confocal Microscopy—The NR8383 cells were grown in culture flasks and treated or not with LPS (InvivoGen, Toulouse, France) at a concentration of 200 ng/ml before being subjected to immunofluorescence studies. For actin immunostaining, the cells were fixed with 4% paraformaldehyde (PFA) for 10 min, washed with PBS, permeabilized with 0.2% Triton X-100 for 10 min at room temperature, blocked with 1% BSA, 1% OVA and 1% normal donkey serum for 1 h and stained with phalloidin labeled with rhodamine (1/100, Santa Cruz Biotechnology, Heidelberg, Germany) at 4 °C for 30 min. After washing with PBS, the nuclei were stained with Hoechst 33342 (1/10000), and the cells were visualized by confocal microscopy. Fluorescence analysis was conducted using a Zeiss LSM 510 confocal microscope (488 nm excitation for Alexa 488 and 543 nm for Alexa 546) connected to a Zeiss Axiovert 200 M with a 63X1.4 numerical aperture oil immersion objective. Both channels were excited, collected separately and then merged to examine the colocalization. The image acquisition characteristics (pinhole aperture, laser intensity, scan speed) were the same throughout the experiments to ensure comparability of the results.

Identification of Cytokines and Chemokines Using Rat Cytokine Antibody Arrays—NR8383-K_D and -NT cells were plated on sterile six-well plates until confluence was attained. The cells were starved overnight with Ham's F12K medium supplemented with 2% FBS and stimulated for 24 h with 20 ng/ml IL-10 (Peprotech) in serum-free medium or left untreated. The medium was then replaced, and the cells were stimulated for 24 h with 200 ng/ml LPS or left untreated. The cell supernatants were collected, centrifuged at 500 × g, passed through a 0.22-μm filter to remove cells and immediately frozen in liquid nitrogen.

The Rat Cytokine Array Panel A from R&D system was used to probe the cytokines in the secretome of stimulated and nonstimulated NR8383 cells by following the procedures recommended by the manufacturer. The membranes were quantified by densitometry using ImageJ software. Statistical analyses were performed using the paired *t* test. Error bars represent the S.E.

Total and Nuclear Protein Extracts—NR8383-K_D and -NT cells were plated on sterile six-well plates until confluent. For LPS stimulation, the cells were starved overnight with Ham's F12K medium supplemented with 2% FBS. The cells were stimulated with 200 ng/ml LPS in serum-free medium or left untreated. At 1 h, 3 h, 6 h (for Western blot analysis), and 24 h (for FASP), the cells were collected, washed once with ice-cold PBS and then lysed with RIPA buffer for total protein extraction (150 mM NaCl, 50 mM Tris, 5 mM EGTA, 2 mM EDTA, 100 mM NaF, 10 mM sodium pyrophosphate, 1% Nonidet P-40, 1 mM PMSF, 1X protease inhibitors). Cell debris was removed by centrifugation (20000 × *g*, 10 min, 4 °C); the supernatants were collected. For the nuclear extracts, NE-PER Nuclear and Cytoplasmic Extraction Reagents were used (Thermo Scientific) according to the manufacturer's instructions. The supernatants were collected, and the protein concentrations were measured using the Bio-Rad Protein Assay.

Western Blot Analysis—The total cell extracts (40 μg) or nuclear extracts (5 μg) were then analyzed by Western blot assays. Primary antibodies were rabbit anti-IRF3, mouse anti-phospho-IκBα, mouse anti-IκBα (1:1000, from Cell Signaling Technology, Leiden, The Netherlands) and rabbit anti-lamin A (1:1000, from Abcam). Horseradish peroxidase-coupled goat antimouse and goat anti-rabbit secondaries (Jackson ImmunoResearch) were used at 1:30000 and 1:20000 respectively. ImageJ software was used to quantify the bands.

Filter-aided Sample Preparation (FASP)—The total protein extract (0.1 mg) was used for FASP analysis as described previously (14). We performed FASP using Microcon devices YM-10 (Millipore) before adding trypsin (Promega) for protein digestion (40 μg/ml in 0.05 M NH_4HCO_3). The samples were incubated overnight at 37 °C. The digests were collected by centrifugation, and the filter device was rinsed with 50 μl of NaCl 0.5 M. Next, 5%TFA was added to the digests, and the peptides were desalted with a Millipore ZipTip device before LC-MS/MS analysis.

Secretome Preparation and Protein Digestion—NR8383-K_D and -NT cells were plated in sterile 24-well plates until confluent. For LPS stimulation, the cells were starved overnight with Ham's F12K medium supplemented with 2% FBS. The cells were stimulated with 200 ng/ml LPS in serum-free medium or left untreated. At 1, 16, 24, 48, and 72 h, the cell supernatants were collected, centrifuged at 500 × *g*, passed through a 0.22-μm filter to remove the cells and immediately frozen in liquid nitrogen. The experiments were performed in biological triplicates.

Four hundred microliters of the secretome was collected for each condition. The volume was reduced to 100 μl in a SpeedVac. Secretome digestion was performed as previously described (15). In brief, the cell supernatants were denatured with 2 M urea in 10 mM HEPES, pH 8.0 by sonication on ice. The proteins were reduced with 10 mM DTT for 40 min followed by alkylation with 55 mM iodoacetamide for 40 min in the dark. The iodoacetamide was quenched with 100 mM thiourea. The proteins were digested with 1 μg LysC/Trypsin mixture (Promega) overnight at 37 °C. The digestion was stopped with 0.5% TFA. The peptides were desalted with a Millipore ZipTip device in a final volume of 20 μl of 80% ACN elution solution. The solution was then dried using the SpeedVac. Dried samples were solubilized in water/0.1% formic acid before LC MS/MS analysis.

LC MS/MS Analysis—The samples were separated by online reversed-phase chromatography using a Thermo Scientific Proxeon Easy-nLC system equipped with a Proxeon trap column (100 μm ID × 2 cm, Thermo Scientific) and a C18 packed-tip column (75 μm ID × 10 cm, Thermo Scientific). The peptides were separated using an increasing amount of acetonitrile (5–35% over 100 min) at a flow rate of 300 nl/min. The LC eluent was electrosprayed directly from the analytical column, and a voltage of 1.7 kV was applied via the liquid junction of the nanospray source. The chromatography system was coupled to a Thermo Scientific Q Exactive mass spectrometer that was programmed to acquire in a data-dependent Top 10 method. The survey scans were acquired at a resolution of 70 000 at *m/z* 400.

Data Analyses—All MS data were processed with MaxQuant (25) using the Andromeda (26) search engine. The proteins were identified by searching MS and MS/MS data against the Decoy version of the complete proteome for Rattus norvegicus in the UniProt database (UniProt Consortium. Reorganizing the protein space at the Universal Protein Resource (UniProt. Nucleic Acids Res. 2012, 40 (Database issue), D71–5.) (Release June 2014, 33675 entries) combined with 262 commonly detected contaminants. Trypsin specificity was used for digestion mode, with N-terminal acetylation and methionine oxidation selected as variable, and carbamidomethylation of cysteines set as a fixed modification. We allowed up to two missed cleavages. For the MS spectra, an initial mass accuracy of 6 ppm was selected, and the MS/MS tolerance was set to 20 ppm for the HCD data. For identification, the FDR at the peptide spectrum matches (PSM) and protein level was set to 0.01. Relative, label-free quantification of the proteins was conducted using the MaxLFQ algorithm (27) integrated into MaxQuant with default parameters. The data sets and Perseus result files used for analysis were deposited at the ProteomeXchange Consortium (*28*) (http://proteomecentral.proteomexchange.org) via the PRIDE partner repository (29) with the data set identifier PXD001984 for cellular extracts (For reviewer access only Username: reviewer62003@ebi.ac.uk; Password: zokVruKN) and PXD001986 for the secretome analyses (For reviewer access only Username: reviewer19925@ebi.ac.uk; Password: PUUJeVfO). Analysis of the identified proteins was performed using Perseus software (http://www.perseus-framework.org/) (version 1.5.0.31). The file containing the information from the identification and hits from the reverse database were used, and proteins with modified peptides and potential contaminants were removed. The LFQ intensity was logarithmized (log2(x)). Categorical annotation of the rows was used to define the different group depending on the following: (1) the cell line (NT or K_D); (2) the treatment (Ctrl/LPS); and 3) the kinetics of the secretomes (1 h, 16 h, 24 h, 48 h, or 72 h). Multiple-sample tests were performed using ANOVA with a FDR of 5% and preservation of the group randomization. To evaluate the enrichment of the categorical annotations (Gene Ontology terms and KEGG pathway), Fisher's exact test was performed taking in account the results of the ANOVA for each group. Normalization was achieved using a Z-score with matrix access by rows. Only proteins that were significant by ANOVA were used for the statistical analysis. Hierarchical clustering was first performed using the Euclidean parameter for the distance calculation, and the average option for linkage in the rows and columns of the trees was used with a maximum of 300 clusters. To quantify fold changes in proteins across the samples, we used MaxLFQ. To visualize these fold changes in the context of individual protein abundances in the proteome, we projected them onto the summed peptide intensities normalized by the number of theoretically observable peptides. Specifically, to compare the relative protein abundances between and within samples, the protein length normalized to the log 2 protein intensities (termed the "iBAQ" value in MaxQuant) was included in the MaxLFQ differences. Functional annotation and characterization of the identified proteins were performed using PANTHER software (version 9.0, http://www.pantherdb.org) and STRING (version 9.1, http://string-db.org). The GeneMANIA Cytoscape plugin (30) was used to generate co-expression networks from cell extracts proteomics data. A "basal" network composed of 95,886 recognized interactions was generated from the data obtained by the analysis of K_D or NT cells under basal conditions. A supervised clustering was then performed to identify the top 100 molecules that coregulated with Anxa6 in this "basal network." The list of 100 genes which encoded molecules were identified was then assessed for gene set enrichment using EnrichR (31) and the GO classification. Following the same approach, two "LPS-stimulated" networks were then generated from the data obtained by the analysis of: (1) unstimulated or LPS-stimulated K_D cells (89,017 recognized interactions) and (2) unstimulated or LPS-stimulated NT cells (96 563 recognized interactions). A supervised clustering was then performed to identify the top 100 molecules that coregulated with NFKB1 in each of these "LPS-stimulated" networks. Both lists of 100 genes that encoded molecules were identified and then assessed for gene set enrichment using EnrichR and the GO classification. Finally, subnetworks of genes presenting significant enrichments for specific GO terms were selected and visualized on Cytoscape. For presentation purposes, nodes were assigned equal weights and subnetworks were slightly distorted to avoid nodes superimposition.

Systems Biology Analysis—The altered pathways relevant to overexpressed proteins in K_D PC1/3 cells were analyzed using Pathway Studio software v.10 (Ariadne Genomics, Rockville, MD). This soft-

ware helps to interpret biological meaning based on gene (protein) expression, to build and analyze pathways, and to identify relationships among genes, proteins, cell processes, and diseases. This software contains a built-in resource named ResNet, which is a database of molecular interactions based on natural language processing of scientific abstracts in PubMed. Using ResNet, a researcher can analyze the gene product/protein list and build a pathway using well-known interactions that are discussed in the existing literature. The program searches the current pathway database and ResNet for interactions with the selected entities and then adds them to the pathway. After the new pathway was constructed, we were able to obtain more detailed information regarding the putative pathways that were altered in response to LPS treatment.

Data Analysis of Mouse Peritoneal Macrophages—An analysis of previously publish data was done to obtain information concerning modifications of proteins induced in peritoneal macrophages from wild type (WT) or PC1/3 KO (KO) mice challenged by LPS (8 h) or not (10). Briefly, peritoneal macrophage from wild type (WT) and PC1/3 knocked out (KO) mice were collected as described previously (10). Cytosolic and membrane fractions were then prepared according to (16) and processed for Gel-LC-MSMS as described in 10. The resulting tryptic peptides were purified and identified by reversed-phase chromatography coupled to an LTQ-Orbitrap Velos (Thermo Scientific). For identification, raw files were filtered for high quality spectra and converted to mgf files using scaffold software (4.4.5) (17) and analyzed using ProteinPilot software 4.5 (18). For each samples all gel band of a particular condition were combined for protein identification. FDR was calculated using PSPEP files (Sciex) and protein alignment was done with the protein alignment template 2.0 (Sciex) using a local protein FDR of 95% (19) over a combined list of all identified proteins. Only proteins with a score of over 6, which represents the proteins identified with two or more unique peptides and at least a fold change of 4 (converted log2 value) were kept for analysis. The relative protein expression was calculated based on the protein score, which was shown to be an adequate relative indicator of the relative differential expression (20). Ratio between WT and KO was calculated using the sum of corresponding fractions. Gene ontology analysis was performed using Blast2go (21).The network analysis was performed as follows: The gene names of identified proteins were used as input to retrieve a network from STRING (22), and this network was then loaded into Cytoscape 3.2 (23, 24). with relative expression data using Id mapper. The Reactome FI pluggin was used to select a subnetwork of gene ontology terms and NCI database-associated specific proteins

Calcium Imaging—Cells were plated onto glass coverslips and loaded with 4 μM Fura-2 AM at room temperature for 45 min in growth medium. Recordings were performed in HBSS containing the following: 140 mM NaCl, 5 mM KCl, 2 mM $MgCl_2$, 0.3 mM Na_2HPO_3, 0.4 mM KH_2PO_4, 4 mM $NaHCO_3$, 5 mM glucose, and 10 mM HEPES adjusted to pH 7.4 with NaOH. The cells were then washed three times in HBSS. The fluorescence intensity of Fura-2 in each cell was monitored and recorded at 340 and 380 nm. To represent the variation in the intracellular free calcium concentration, the fluorescence intensity ratio represented by F340/F380 was used as an indicator of the changes in cytosolic Ca^{2+} concentrations.

Isolation of Human Immune Cell Subsets for the Migration Assay—Human blood samples were collected from healthy adult donors with informed consent obtained in accordance with Institutional Review Board approval from the Institut de Biologie de Lille. Mononuclear cells (PBMCs) were isolated from peripheral blood samples by density gradient centrifugation using Ficoll. Human NK, CD8+ and $CD4^+CD25^-$ conventional T cells were purified from PBMCs by magnetic separation using NK and T cell isolation kits as described by the manufacturer (Miltenyi Biotech, Bergisch Gladbach, Germany). The purity of the isolated NK, $CD8^+$, and $CD4^+$ T cells was >95%. NK cells were activated using recombinant IL-2 (200 UI/ml, BD Pharmingen, San Jose, CA) and IL-15 (200 UI/ml, BD Pharmingen). $CD8^+$ and $CD4^+$ T cells were activated with plate-bound anti-CD3 (1.5 μg/ml, Clinisciences, Nanterre, France) antibody and incubated at 37 °C for 2 h prior to culturing. Soluble mouse anti-human CD28 antibody (100 ng/ml, Clinisciences) was added to the cells at the time of culture.

Migration Assay—The different NK and T cell populations were harvested and suspended at a concentration of 10^6 cells/ml in RPMI 1640. The chemotaxis protocol was performed as previously described (32) using a 48-well microchemotaxis Boyden chamber with 5-μm pore polycarbonate filters. The cells were incubated for 2 h 30 min at 37 °C in 5% CO_2 with NR8383 secretomes (NT and PC1/3-K_D nonstimulated or stimulated with 200 ng/ml LPS for 24 h). Each condition was performed in triplicate. Cells that migrated through the filter were counted in the inferior well. The results are expressed as the number of activated cells that were attracted by each secretome compared with the nonactivated ones.

Cell Viability Measured by the CellTiter-Glo Assay—SKBR3 and SKOV3 cells were seeded into 96-well white plates (6500 and 3000 cells per well, respectively) with NR8383 secretomes obtained after 24 h of LPS stimulation or no stimulation. The assay was conducted for 24, 48, 72, or 96 h. For the 96 h+ medium, conditioned secretomes were removed at 72 h and replaced with fresh ones. CellTiter-Glo reagent (Promega) was added to the wells and incubated at room temperature for 10 min protected from light. The luminescence was recorded using a Berthold luminometer Centro LB960. The results are expressed as relative light units (RLUs).

RESULTS

PC1/3-knockdown NR8383 Cells Express an Inflammatory Profile—A stable PC1/3-K_D cell line has been developed by lentiviral delivery of shRNAs (11). To better understand the interaction and regulation of TLR4 by PC1/3, we used these PC1/3-K_D NR8383 cells in the present study. A proteomics analysis was performed to identify secreted proteins subsequent to PC1/3 silencing in NR8383 cells, before and after LPS challenge. Shotgun proteomics of secreted proteins (from 1 h to 72 h after stimulation) was performed for nontarget (NT) control cells and K_D cells (Fig. 1). More than 1400 proteins were identified in all analyses of the NR8383 secretomes (supplemental Data S1).

Comparison of the identified proteins between resting K_D or NT cells and cells challenged with LPS allowed the identification of 28 specific proteins that were directly related to PC1/3 (Fig. 1*A*). These proteins were only secreted by K_D cells, both resting and those stimulated with LPS. The proteins are involved in different functions, *e.g.* responses to stimuli, RNA processing, endocytosis, regulation of transcription, catabolism, protein binding, regulation of axogenesis and immune responses (Table I).

This study was then further coupled to a kinetic study at 1 h, 16 h, 24 h, 48 h, and 72 h after LPS challenge. Proteins with an abundance that was significantly different among the conditions were determined according to the MaxQuant and Perseus software. As a criterion of significance, we applied an ANOVA significance threshold of $p < 0.05$, and heat maps were created. A total of 125 proteins in the cell culture super-

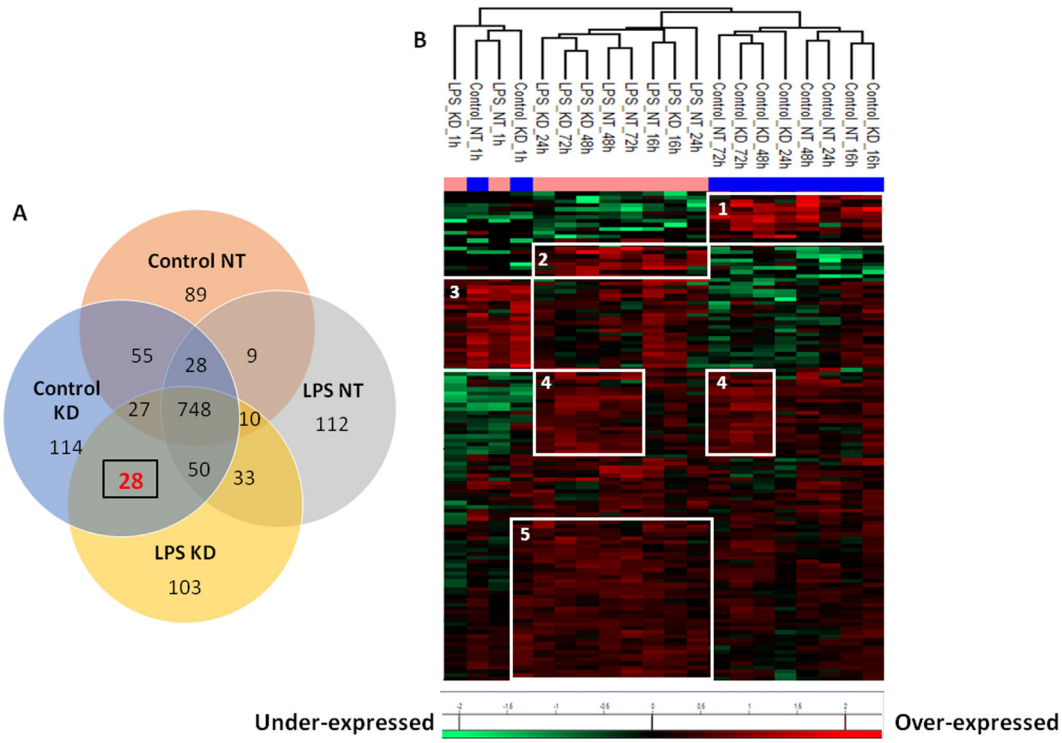

FIG. 1. **Secretome analysis strategy.** *A*, NR8383 cells were stimulated with LPS or were nonstimulated (control), and the supernatants were collected (from 1 h to 72 h). After the proteomic approach, the samples were analyzed by LC-MS/MS. The numbers of identified secreted proteins found in common or specific for K_D and NT macrophages (nonstimulated or stimulated with LPS) are represented in a Venn diagram. Twenty-eight proteins were specific to the PC1/3 K_D. *B*, Heat map of proteins with different secretion profiles in NR8383 macrophages stimulated with LPS *versus* nonstimulated (control). Distinct clusters are highlighted.

natants of the macrophages stimulated with LPS *versus* nonstimulated macrophages were considered reliable based on the statistical analysis (Fig. 1*B*, supplemental Data S2).

Two major branches of the heat map separate the 1-h series from the other time points. In the second branch, two branches distribute the control *versus* the stimulated cells. Each experiment was performed 3 times, and each sample corresponded to the statistical data obtained per condition. Five specific clusters of over-expressed proteins were retrieved. Cluster 1 is specific to the control (16 h–72 h). Clusters 2 and 5 are specific to LPS stimulation (16 h–72 h). Cluster 3 represents proteins found after 1 h in both control and LPS-stimulated cells. Cluster 4 is specific to later time points (48 h and 72 h). For each cluster, proteins with specific functions were characterized. For example, in cluster 2, proteins implicated in macrophage activation and the immune response were specific to LPS stimulation. In cluster 1, the majority of the proteins were implicated in protein synthesis associated with early stimulation. The complete list of proteins in these clusters is provided in Table II.

Among the proteins identified in clusters 4 and 5 (Table II) were the alarmins (*e.g.* GRP78, HSP84, HSP86, HSP73, calreticulin, capthepsin B, nucleolin, and granulins)(33). Alarmins are produced by immune cells through the endoplasmic reticulum (ER)-Golgi secretion pathway and are involved in triggering the adaptive immune response. Analyses of the other clusters revealed the release of chemokines (CXCL10 and CCL3), cytokines (MIF), interferon-inducible protein (IFI30) and growth factor (GDF15). Both chemokines and alarmins have known functions in immune responses. These proteins recruit and activate receptor-expressing cells of the innate immune system, including dendritic cells and CD4+ cells, and they also directly or indirectly promote adaptive immune responses (34).

To analyze the chemokine/cytokine pattern between NT and K_D PC1/3 NR8383 cells in detail, time course analyses of chemokine and cytokine protein expression were performed without quantification (Fig. 2*A*).

Both nonstimulated and challenged K_D cells secreted CCL3, CCL6, CCL9, CXCL10, CXCL2, MIF, and IL-1RA. Challenged K_D cells also secreted CCL7, CCL2, and CXCL3. Comparisons with NT cells revealed that most chemokines were released by both cell types. However, differences in the timing and nature of the secreted chemokines were evident. CXCL3 was only secreted by K_D cells, whereas the inhibitory chemokine TGF-β was secreted by NT cells. MIF protein was not secreted by NT cells in response to LPS stimulation. To validate these results and to quantify the chemokine and cytokine levels released by NR8383 cells, cytokine arrays were performed after 24 h of stimulation (Fig. 2B). As shown, NR8383

TABLE I
List of 28 secreted proteins specific to PC1/3 knockdown from Figure 2A

Protein Name	Biological Function
Protein Arap1	Response to stimuli, signal transduction
Choline-phosphate cytidylyltransferase A	
STE20-like serine/threonine-protein kinase	
Mitogen-activated protein kinase 14	
Inositol polyphosphate-1-phosphatase	
Paired immunoglobulin-like type 2 receptor alpha	T cell activation, regulation of inflammatory responses
Galectin-1	
Protein Vnn1	
Insulin-like growth factor-binding protein 2	
Heterogeneous nuclear ribonucleoprotein M	RNA processing
DEAH box polypeptide 9	
Protein Ddx6	
rRNA 2′-O-methyltransferase fibrillarin	
Mitochondrial import inner membrane translocase	Protein folding and localization, endocytosis
Protein Txndc5	
Peptidyl-prolyl cis-trans isomerase	
Vacuolar protein sorting-associated protein 26A	
Protein RGD1309995	
UDP-glucose:glycoprotein glucosyltransferase 1	
H2-K region expressed gene 2	
ATPase Asna1	
Canopy 2 homolog	Regulation of transcription
Protein Cbx1	
Protein Raly	
Phospholipase A2	Catabolic processes
Xaa-Pro dipeptidase	
Protein Ubap21	Protein binding
Reticulon-4	Regulation of axonogenesis

cells secreted several chemokines, including CCL5, CCL3, CXCL9, CCL20, CXCL10, CXCL1, and CXCL2. We established that without LPS challenge, NR8383 K_D cells produced significantly more CCL5, CXCL1, CXCL2, CXCL10, IL-6, and TNF-α than NT cells (Fig. 2*B*). Moreover, following LPS challenge, K_D cells additionally produced CXCL9 and CCL20 and concomitantly released the previous cytokines and chemokines CXCL1, CXCL2, CXCL10, IL-1α, and IL-1β. These chemokine and cytokine profiles are characteristic of secretion through the unconventional secretory pathway, which involves synthesis in the cytoplasm and release without passing through the ER and Golgi complex (35).

PC1/3-K_D NR8383 Cells and Modulation of the Intracellular Trafficking Machinery—Members of the IL-1 cytokine family, particularly IL-1α and IL-1β are key inflammatory cytokines that are released through the unconventional secretory pathway. Unconventional vesicular or organellar pathways have been discussed. To determine whether the secretory pathway is affected by PC1/3 K_D, proteomic studies of the cellular contents were undertaken in NT and K_D cells under either resting conditions or at 24 h post-LPS stimulation (Fig. 3, supplemental Data S3). For the ANOVA test, the samples were classified between NT and K_D. Two clear clusters were highlighted. Cluster number 1 represents over-expressed proteins in K_D cells, whereas cluster number 2 groups over-expressed proteins in NT cells (Fig. 3*A*, Table III and supplemental Data S4). The proteins in each cluster were then analyzed using PANTHER software (http://www.pantherdb.org) to determine the biological functions based on the protein classes. Using this analysis, we demonstrated that over-expressed proteins in K_D cells were implicated in cell adhesion, extracellular matrix or cytoskeleton, whereas in NT cells, over-expressed proteins were involved in nucleic acid binding or oxidoreduction functions (Fig. 3*B*). For a more detailed analysis, we performed a systems biology analysis for network identification of the over-expressed proteins in PC1/3-K_D cells (Fig. 3*C*). Differential pathways were generated using the "direct interaction" algorithm to map the relationships of the identified proteins (supplemental Data S5). We found that among the 85 altered proteins, 32 proteins had direct regulatory relationships, including binding, post-translational modifications and transcriptional regulation. Different biological processes are represented by the over-expressed proteins in PC1/3 K_D cells (Fig. 3*C*). For instance, these proteins are involved in actin organization, inflammatory responses, cytoskeletal assembly, T cell activation and calcium channels. Several of the identified proteins were clustered under certain functional classes, such as cellular remodeling (Cluster 1, supplemental Data S5), immune activation and calcium export (Cluster 2, supplemental Data S5), which is consistent with the

TABLE II
List of proteins identified in specific clusters after Perseus analyses from Figure 2B and Supplementary data 2

Cluster 1	Cluster 2	Cluster 3	Cluster 4	Cluster 5
Alcam	Sqstm1	LOC685186	Rplp2	Hspa8
Mif	Marcks	Eef2	P4hb	Atic
Lpl	Sdc4	Txn	Hspa5	Aldoa
Ifi30	Cxcl10	Pgk1	Ncl	Pygl
Smpdl3a	Ccl3	Tcp1	Calr	Rpl5
Gpnmb	Hn1	Ywhab	Vim	Cltc
Ganab	Ndrg1	Rhoa	Fabp5	Pkm
Fkbp2	Gdf15	Eef1a1	Arhgdia	Hsp90ab1
Axl		Gm15013	Tpm3	Cfl1
Lyz2		Ran	Hnrnpa3	Vcp
Ctsd		Gnb2l1	Prdx5	Tpi1
Npc2		Actg1	Prg4	Tkt
		Ywhaq	Calu	Gdi2
		Clic1	Akr1b8	Ywhag
		Tuba1b	Grn	Rps11
		Cdc42	Ahnak	Tmsb4x
		Rpl7	Ctsb	Atp6v1b2
		Cct8	Tpm4	Ywhah
		Tubb4b	Eef1b2	Hsp90aa1
		Ugp2		Pgd
		Eif4a1		Cap1
		Rpl4		Vat1
				Eif5a
				Actr3
				Cct2
				Prdx1
				Myl6
				Eef1d
				Cndp2
				Cct4
				Pdcd6ip
				Flna
				Atp6v1a
				Cct7
				Msn
				Kpnb1
				Iqgap1
				Tln1
				Cct6a

results obtained using PANTHER software analysis (Fig. 3*B*). Further demonstrating the impact of PC1/3 K_D on the cytoskeleton organization, we found that molecules co-up-regulated with Anxa6 in K_D cells were highly significantly related with the GO terms "actin binding" or "extracellular vesicular exosome" (Fig. 4*A*).

Next, we focused on proteins that are important for the cytoskeleton (Table III). Among these cytoskeletal proteins, STRING analysis revealed that most of them are known to be involved in the ARP2/3 complex and the WAVE complex (WASF2, ACTR3, ARPC1B) (supplemental Data S6). Wiskott-Aldrich syndrome protein (WASP) is known to lead to upstream signals resulting in activation of the ARP2/3 complex, which causes a burst of actin polymerization and the formation of a lamellipodium structure. ARP2/3-complex-mediated actin polymerization is crucial for the reorganization of the actin cytoskeleton at the cell cortex during processes such as cell movement and vesicular trafficking (36). Moreover, macrophage activation promotes changes in macrophage cell elasticity that depend on actin polymerization. Cytoskeletal rearrangements are observed between activated and nonactivated macrophages: activated macrophages are elongated, whereas nonactivated cells are more circular (37).

To validate our hypothesis regarding cytoskeletal rearrangements, we incubated NR8383 macrophages with phalloidin to stain the actin filaments. We clearly demonstrated that resting PC1/3-K_D cells were more elongated and expressed a high level of directional actin-filled structures compared with NT cells (Fig. 4*B*a and b). In this context, PC1/3-K_D cells were polarized, with long actin filopodia that emanated from one side of the cell and actin-associated membrane

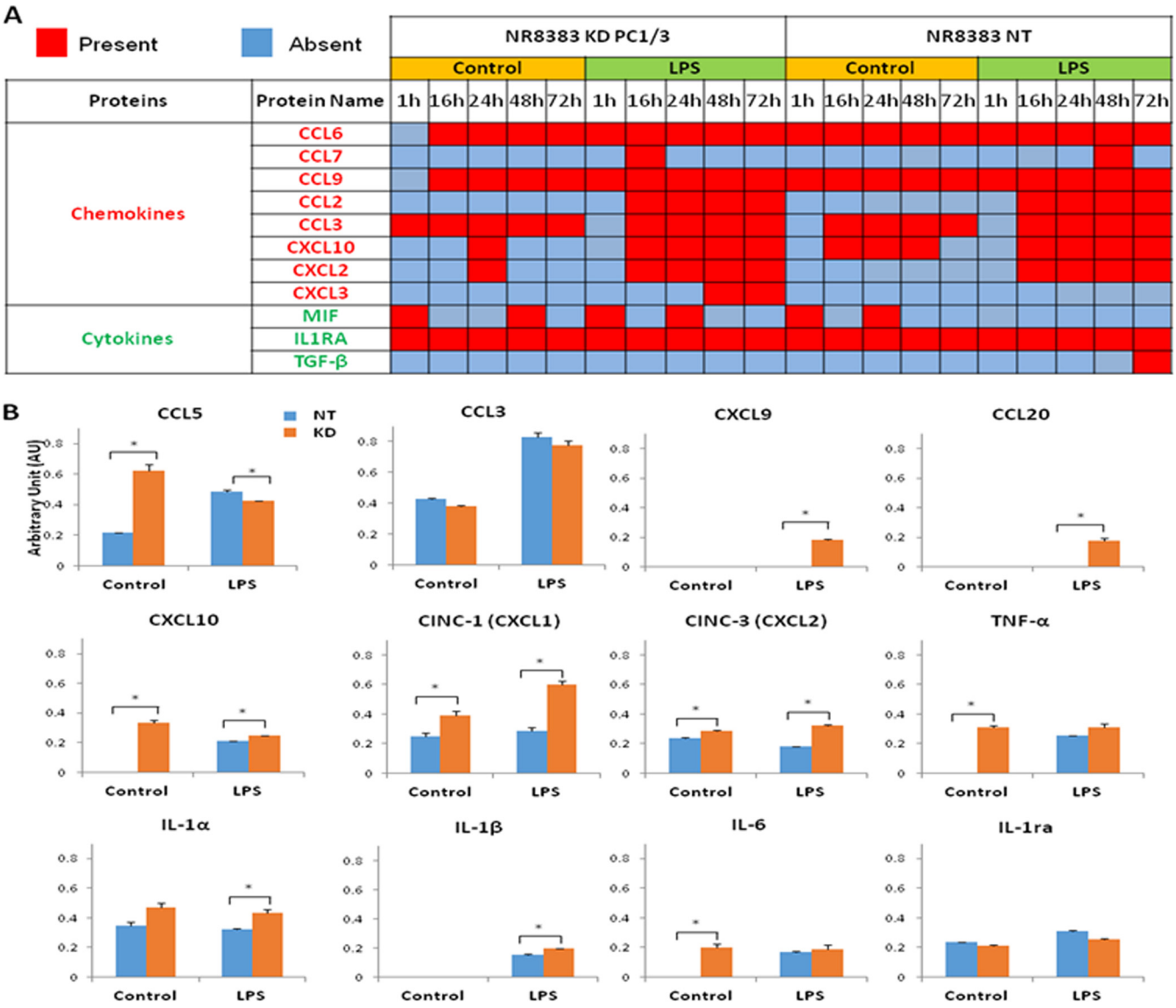

FIG. 2. **Chemokines and cytokines secreted by NT and K_D cells over the time that were challenged or not with LPS.** *A*, Mass spectrometry analyses allowed for the identification of chemokines and cytokines over time. For identification, FDR was set at 0.01. Blue indicates proteins that were absent, whereas red shows proteins that were present in the secretome. *B*, Rat cytokine array assay. Cells were untreated (control) or treated with LPS for 24 h. The NT cell secretomes are shown in blue, and the K_D cell secretomes are in orange. The bar diagrams represent the ratio of the spot mean pixel densities/reference point pixel densities. Significant differences were analyzed using Student's *t* test. $^*p < 0.05$.

ruffling on the other side (Fig. 4*B*b). Thus, PC1/3-K_D cells expressed an activated phenotype, and, in response to LPS challenge, the number of filopodia increased corresponding to a higher level of activation in these cells (Fig. 4*B*c and d). Filopodia in LPS-stimulated NT cells increased as compared with control cells demonstrating an activation state under LPS. These results are consistent with the data obtained using proteomics for cytoskeletal reorganization (Figs. 3 and 4*A*).

It has been shown that the cytoskeleton regulates cell polarity, migration and cytokine secretion via vesicular trafficking. Based on the proteomic data, proteins specific to Golgi vesicle transport were clearly under-expressed in K_D cells (Table IV).

Among them, we found the following proteins in the same cluster: STX7, USO1, NSF, and COPG1. These proteins are required for transport from the endoplasmic reticulum to the Golgi stack (38) and catalyze the fusion of transport vesicles within the Golgi cisternae. By contrast, endosome-specific proteins (early, late, recycling) APPL1, VAC14, EHD4, VPS4B, ANXA6, and RAP2B and GGA2 proteins involved in protein trafficking between the trans-Golgi network (TGN) and endosomes were over-expressed in K_D cells (Table IV). These

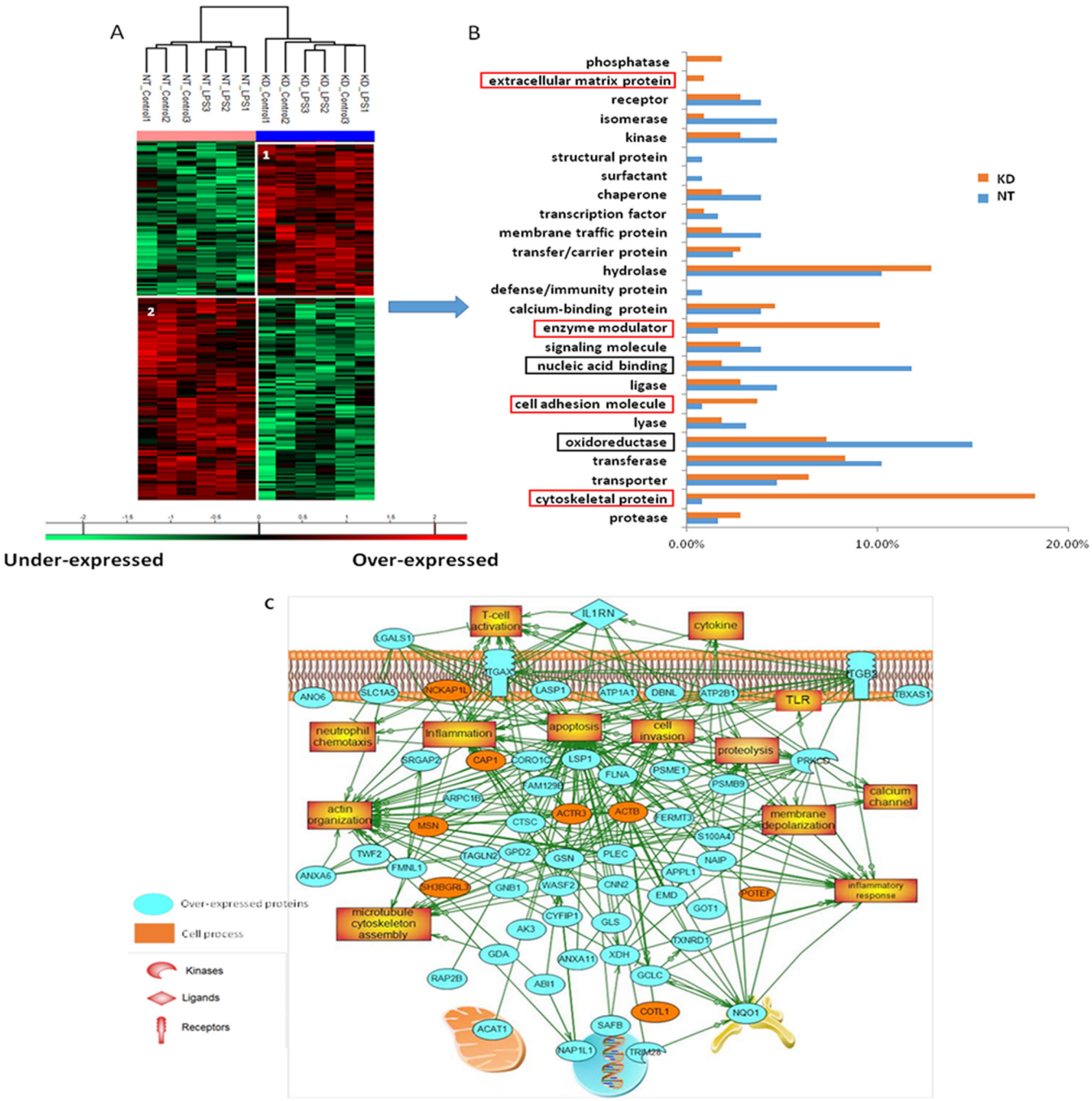

FIG. 3. **Whole-cell extract analysis strategy.** *A*, NR8383 cells were stimulated with LPS (200 ng/ml) or not (control) and lysed before FASP and LC-MS/MS analysis. MaxQuant and Perseus software were used for the statistical analysis, and a heat map was generated to show proteins that were significantly different between NT and PC1/3-K_D NR8383 macrophages in the cell extracts. Two clusters are highlighted. *B*, The proteins in each cluster were analyzed using Panther software. The biological functions associated with these proteins are shown. The functions framed in red correspond to those of proteins that were over-expressed in K_D cells, whereas the functions framed in black correspond to those of proteins that were over-expressed in NT cells. *C*, Global pathway analysis of the over-expressed proteins identified in PC1/3-K_D cells. Over-expressed proteins in PC1/3-K_D cells were involved in global altered molecular pathways. The different colors reflect the degree of expression. Proteins in blue are over-expressed in PC1/3-K_D cells, whereas those in orange show no expression differences between NT and K_D cells.

proteins are required for the regulation of cell proliferation in response to extracellular signals from an early endosomal compartment and also play a role in the biogenesis of endosome carrier vesicle (ECV)/multivesicular body (MVB) transport intermediates from early endosomes (38). Moreover, these proteins are involved in the late steps of the endosomal

TABLE III
List of proteins identified in specific clusters after Perseus analyses from Fig. 3A and supplementary Data S4

Cluster 1			Cluster 2		
LOC684352	Lgals1	Slc1a5	Fcgr2b	Hspa5	Ephx2
Cotl1	Got1	Bpnt1	Colgalt1	Eno2	Aldh3b1
Acad9	Gls		Rpl22l2	Manf	Ogdh
Fermt3	Gclc		Acad11	Acaca	Aarsd1
Fam129b	Il1rn		Uap1l1	Pdia3	Pdk1
Flna	Plec		Sh3bgrl	Ncl	Nucb1
Nckap1l	Gpd2		Ganab	Etfa	Camk1
Atp2b1	Acadvl		Hist1h1b	Anxa3	Cd14
Fmnl1	Anxa6		Ktn1	Pgk1	Aldh7a1
Nmral1	Tbxas1		Cul4b	Ppib	Atg7
Naip5	Pdhb		Ube2m	Pgam1	Npl
Gsdmd	Gnb1		Plod1	Scarb2	Nasp
Cnn2	Rap2b		Eif4g1	Aldh1l1	Snd1
Itgax	Ctsc		Siglec1	Psmb6	G3bp2
Srgap2	Ctbs		Usp5	Pfkl	Atp6v1d
Ahcyl1	Nit2		Naglu	Pebp1	Gpi
Vsig8	Vps4b		Atp6v1a	Uso1	Nampt
Cyfip1	Lsp1		Apobr	Idh1	Ero1l
Anxa6	Actr3		Fam120a	Tpi1	Pcyox1
Cct8	Wdr1		Rab32	P4ha1	Cth
Ipo7	Tagln2		Hyou1	Prkaa1	Fam129a
Wasf2	Anxa11		Fdps	Timm10	Slc9a3r1
Msn	Ech1		Hexb	Vamp3	Bche
Xdh	Adk		Slc25a13	Dnaja1	Uggt1
Slc25a12	Gsn		Dst	Phb	Fkbp4
Ano6	Tuba3a		Gale	Fabp4	Dnajc3
Itgb2	Psmb9		Calu	Eif2s3	Ak4
Coro1c	Ak3		Atp13a1	Ssrp1	Tpmt
Hnrnpd	Psme1		Acly	Eif3a	
Nap1 l1	Emd		Psmd5	Vat1	
Strn	Hdhd2		Aldh3a2	Ddhd1	
Gga2	Cct4		Vav1	Txndc12	
Safb	Vac14		M6pr	Pgm1	
Arpc1b	Ehd4		Gaa	Copg1	
Txnrd1	Lasp1		Stx7	Creld2	
Nqo1	Dbnl		Por	Fam162a	
Atp1a1	Sfxn3		Ldha	Creld1	
Prkcd	Gda		Gapdh	Ufm1	
Aldh4a1	Abi1		Aldoa	Lpcat3	

MVB pathway. MVBs contain intraluminal vesicles that are generated by the invagination and scission from the limiting membrane of the endosomes and are mostly delivered to lysosomes, enabling the degradation of membrane proteins. This phenomenon indicates that PC1/3 K_D remodels the endosomal compartment, which is consistent with our data obtained using macrophages isolated from PC1/3-KO mice. Ontogenic enrichment of proteins issued from our previous publish proteomic analyses of peritoneal macrophages (10) from wild type (WT) or PC1/3 KO (KO) mice challenged by LPS (8 h) or not, confirms the over-expression of cytoskeleton proteins as well as GTPase activity (5 Go terms) (Fig. 5*A*). STRING analysis of proteins with GTPase activity has been performed and the network subsequently analyzed using the visualization tool Cytoscape followed by the Integrated Reactome FI analysis tool which selects subnets with specific ontogenetic functions. The biological interaction network GTPase proteins included 202 proteins. Among the groups of proteins with specific ontogenic functions two groups are overexpressed in KO samples *i.e.* receptor activity and vesicles trafficking. We focused our attention on the last one (Fig. 5*B*). The network consists mainly of small G proteins and Rab proteins responsible for their regulation. The center of the network, the protein Agfg1 (Arf-GAP domain and FG repeats-containing protein (1), has an important role in endocytosis (39) At the periphery of this protein, several Rab show a similar expression profile which is over-expressed in unstimulated KO sub-sample and expressed when stimulated with LPS. These Rab (Rab8, Rab11, Rab14 and Rab27) all have a common function that is exocytosis and secretion (40). This disruption of molecular pathways secretion and the increase of membrane targeted molecules involved in vesicle-associated functions in PC1/3 KO mice (Fig. 5*C*) correlate with dysregulated cytokine secretion as well as intracellular disruption as we found in NR8383 PC1/3 K_D cells. Moreover, these results in both NR8383 PC1/3 K_D cells and PC1/3 KO macrophages are also consistent with the data obtained from the kinetic study of secretion showing a lot of proteins involved in exosomes.

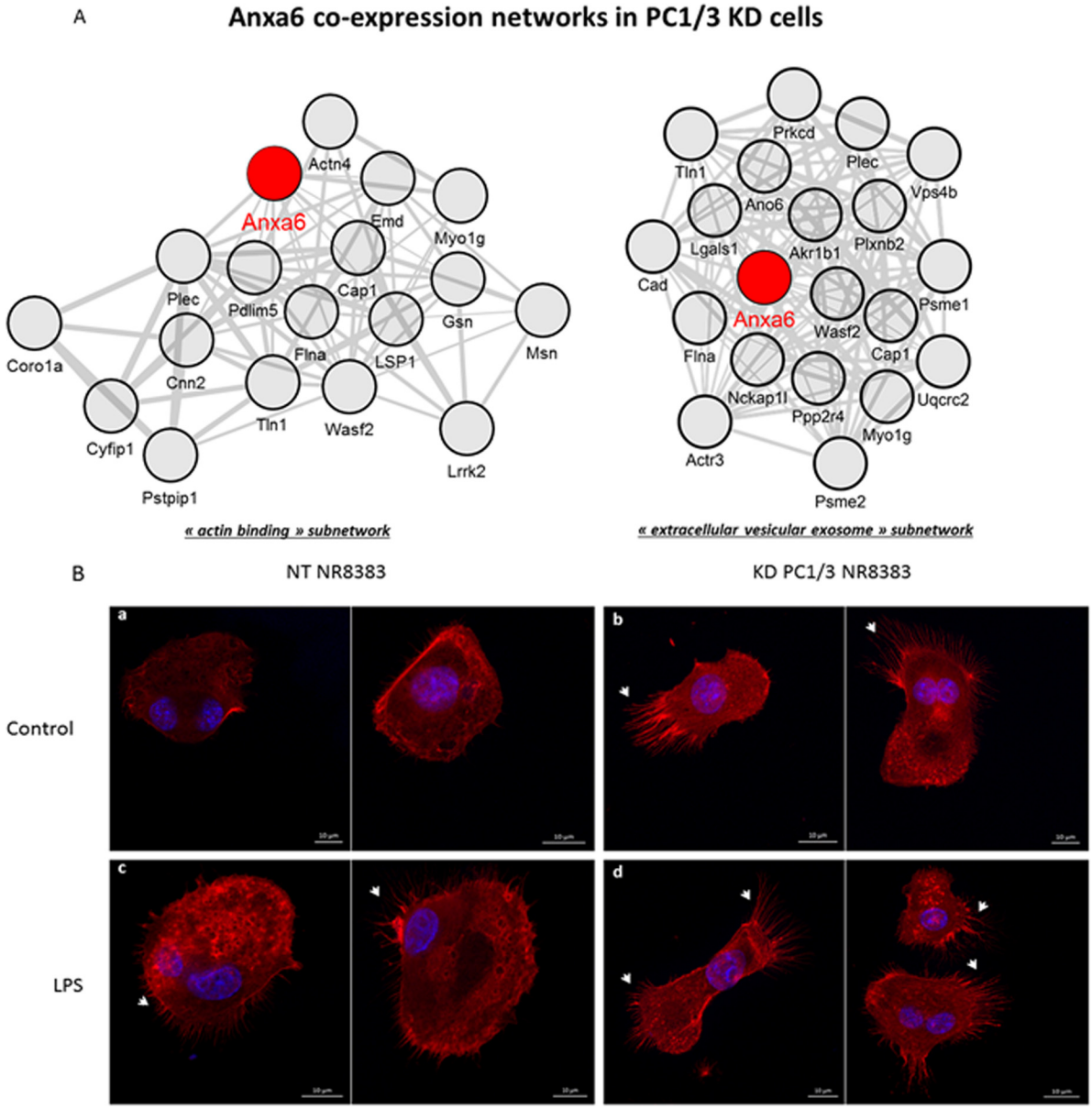

FIG. 4. **PC1/3-K_D cells exhibit cytoskeletal reorganization.** A, Analysis of co-expression network identifies cytoskeletal reorganization in K_D cells. The 100 genes which encoded molecules were the most tightly coregulated with Anxa6 in unstimulated K_D cells were identified and assessed for gene set enrichment. Shown are subnetworks of genes annotated by the GO terms "actin binding" (adjusted p value for enrichment significance = 6.1e-8) (left panel) or "extracellular vesicular exosome" (adjusted p value for enrichment significance = 3.1e-10) (right panel). Only 18 out of 50 genes forming the subnetwork "extracellular vesicular exosome" are shown. *B,* Confocal imaging of NR8383 cells stained with rhodamine-phalloidin (1/100^e). The nuclei were counterstained with Hoechst 33342 (blue). The cells were stimulated with LPS (**c** and **d**) or left untreated (**a** and **b**) for 24 h. Scale bar, 10 μm.

The large amount of inflammatory cytokines produced by the activated PC1/3-K_D cells is consistent with MVB discharge. Interestingly, the cytoskeleton, MVB discharge (38, 41) and Ca^{2+} signaling are linked. Indeed, increasing intracellular Ca^{2+} levels stimulate exosome secretion (41). Moreover, the disruption of actin filaments inhibits Ca^{2+} signaling (42). It has been shown that T cells deficient in WAVE2 and WASP present impaired Ca^{2+} mobilization (43). Gelsolin is another protein that promotes the assembly of actin filaments and has Ca^{2+} binding sites. A low concentration of Ca^{2+} inhibits actin binding, whereas a high Ca^{2+} concentration exposes actin binding sites (44). We have shown that in PC1/3-K_D cells, gelsolin and certain proteins implicated in the WAVE2 and WASP complexes are over-expressed (Table III). Moreover, cytokine secretion is dependent on an increase in intracellular Ca^{2+} (45). The inhibition of store-operated channels (SOCs) leads to a decrease in TNF-α and IL-6 secretion (46). To determine whether calcium homeostasis was impacted in

TABLE IV
List of proteins implicated in the canonical and non-canonical pathway of cytokine secretion

Cellular compartment	Protein name	NT		KO	
		control	LPS	control	LPS
Early endosome	Filamin A	27.3099	26.6311	28.113	27.8758
	DCC-interacting protein 13 alpha	18.3755	18.6619	19.6669	19.7339
	Protein Vac 14	22.4716	21.1599	22.9718	22.4599
	EH-domain containing protein 4	23.5251	22.8681	25.4616	25.3642
	Vacuolar protein sorting associated	22.3025	21.3796	23.1595	22.149
Late endosome	Annexin A6	26.8954	26.0519	27.7486	27.0312
Recycling endosome	Ras-related protein Rap-2b	22.2046	21.6395	23.7746	22.9046
	Vesicle-associated membrane protein 3	26.1284	25.8384	25.4235	24.6955
Golgi vesicle transport	General vesicular transport factor p115	25.111	24.2455	24.2114	23.9002
	Vesicle-fusing ATPase	24.2388	23.3532	23.4758	22.3273
	Syntaxin-7	25.0211	24.8745	23.6678	23.9568
	Coatomer subunit gamma 1	23.9452	23.0883	23.0444	22.6604
Clathrin mediated endocytosis	Sialoadhesin	23.0034	23.3274	19.2157	21.5666
	Twinfilin-2	23.0461	23.0252	23.5662	23.9651
TGN to endosomes	ADP ribosylation factor-binding protein	21.8125	19.7305	23.7937	22.5062

NR8383 cells, we performed calcium imaging experiments (Fig. 6).

For that purpose, we used the calcium probe fura-2AM to evaluate the cytosolic calcium concentration ((Ca^{2+})) in sterile conditions or in response to LPS exposure. We clearly demonstrated that LPS ($n = 3$) rapidly induced a pronounced elevation of (Ca^{2+})c in NR8383-K_D cells compared with NT cells (Fig. 6*A*, 6*B*). Fig. 6*A* shows the Ca^{2+} signals from individual cells, which are quantified in Fig. 6*B*. We next investigated whether other features important for calcium homeostasis were affected in NR8383-K_D cells. Fig. 6*C* shows the quantitative results obtained from original traces of similar Ca^{2+} imaging experiments. Resting (Ca^{2+})c levels were significantly increased in NR8383-K_D cells. To more thoroughly investigate how the (Ca^{2+})c in NR8383-K_D cells was affected, we examined two key processes that determine the basal (Ca^{2+})c in cells. First, we measured store-operated calcium entry (SOCE) mediated by SOCs. SOCs are located in the plasma membrane and are activated by depletion of the internal Ca^{2+} store in response to stimulation of the surface receptor-coupled signaling pathway (47). Ca^{2+} entry mediated by SOCE directly influences (Ca^{2+})c. New intracellular Ca^{2+} imaging experiments were conducted using the SERCA pump inhibitor thapsigargin (TG) as a store-depleting agent (48). As expected, the addition of 2 mM extracellular calcium to NR8383 cells that had been pre-incubated for 10 min with TG (1 μM) in Ca^{2+}-free medium to achieve complete ER Ca^{2+} store depletion resulted in marked and sustained elevation of the (Ca^{2+})c because of the activation of SOCE (Fig. 6*D*). The peak (Ca^{2+})c elevation in relation to SOCE increased by ~70% in K_D NR8383 cells (Fig. 6*E*). Moreover, an increasing (Ca^{2+}) in the bathing solution from 0 mM to 2 mM produced more significant elevations of the basal (Ca^{2+})c in K_D NR8383 compared with NT cells (Figs. 6*F*, 6*G*). Notably, we observed higher resting (Ca^{2+})c levels in NR8383-K_D cells compared with NT cells at normal 2 mM external Ca^{2+} concentrations prior to the application of TG (Fig. 6*F*). This finding suggests that the PC1/3 K_D also promoted enhanced basal Ca^{2+} influx and not only SOCE. The application of TG in the presence of 2 mM extracellular calcium clearly showed that SOCE was not sustained in control cells compared with NR8383-K_D cells. Taken together, these results demonstrate that the basal (Ca^{2+})c increased in K_D NR8383-K_D cells in relation to SOCE and the increase in the constitutive Ca^{2+} influx, which is consistent with the results obtained for the cytoskeletal rearrangements and cytokine release in these cells.

PC1/3-K_D NR8383 Cells and the TLR4 Intracellular Signaling Pathway—As shown previously, in response to LPS treatment, PC1/3 and TLR4 colocalize in the endosomal compartment (11). In PC1/3-K_D cells, this compartment is disorganized (10, 11) (Table IV), and uncontrolled cytokine secretion is observed following LPS stimulation (10). Altogether, these results indicate that PC1/3 or its products may contribute to the regulation of TLR4 signaling. Proteomic data for the cellular extracts allowed us to focus on proteins implicated in immune system responses, particularly TLR signaling (Table V, supplemental Data S3).

LPS stimulation of TLR4 results in the activation of MyD88-dependent signaling and subsequently NF-κB signaling activation. TLR4 can also mediate the activation of MyD88-independent signaling after its internalization leading to the activation of interferon response factor (IRF) 3 (4). It appears that proteins involved in TLR4 signaling were modulated in NR8383-K_D cells. Most importantly, the relative abundance of IRF3 decreased, whereas that of NF-κB1 (also known as p105) increased (Table V). This finding demonstrated that NF-κB was solicited rather than IRF3 and, thus, suggested that the TLR4 MyD88-dependent pathway was activated in K_D cells. Detailed analyses of the results reinforced this hypothesis (supplemental Data S3). Indeed, we observed an over-expression of interleukin-1 receptor accessory protein

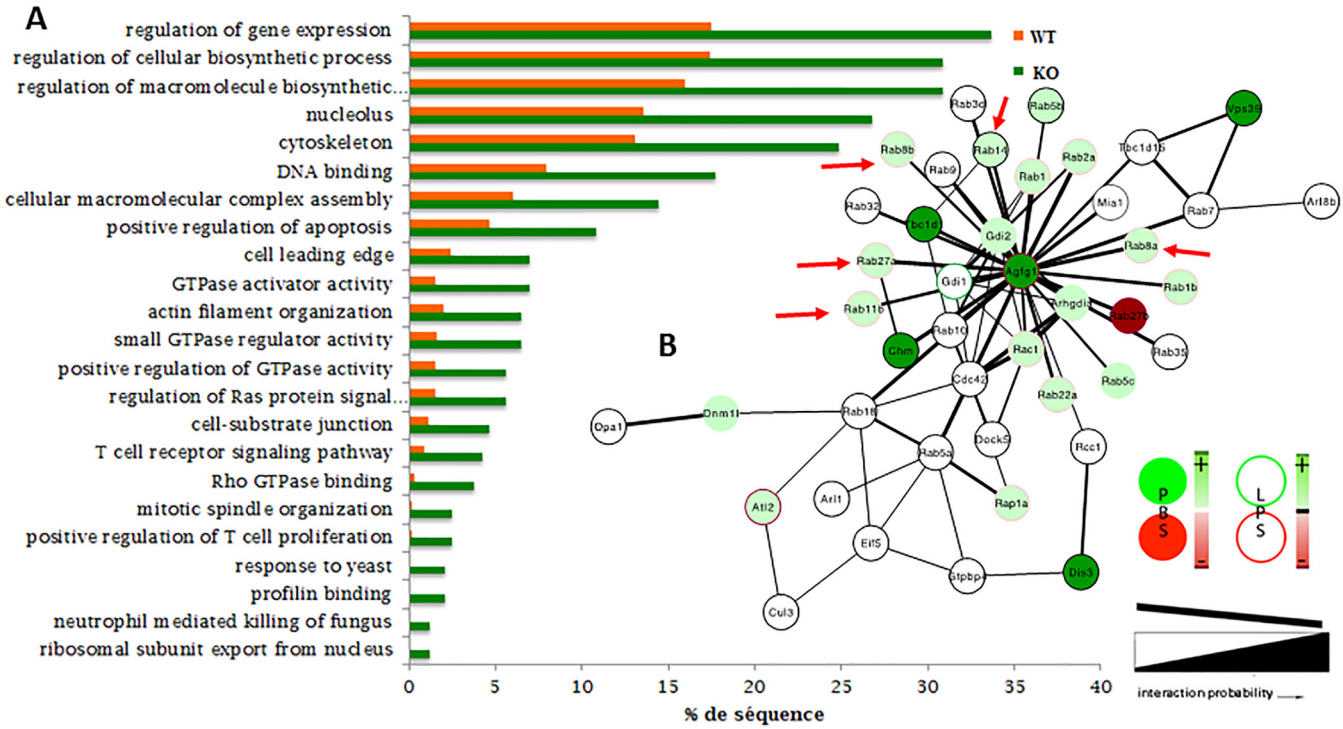

C

	KO-specific membrane-targeted molecules	
	N	Enrichment analysis
Unstimulated macrophages	428	"extracellular vesicular exosome" p = 1.75E-11
LPS-stimulated macrophages	493	"post-Golgi vesicle-mediated transport" P = 0.009

FIG. 5. **PC1/3 KO (KO) mice challenged by LPS exhibit disruption of molecular pathways secretion correlates with dysregulated cytokine secretion.** *A*, Ontogenic enrichment of proteins issued from proteomic analyses of peritoneal macrophages from wild type (WT) or PC1/3 KO (KO) mice challenged by LPS (8 h) *B*, Cytoscape followed by the Integrated Reactome FI analysis tools focus on vesicles trafficking has been realized. The network consists mainly of small G proteins and Rab proteins responsible for their regulation. Color code corresponds to : green over-expressed, red under-expressed of the selected proteins (KO *versus* WT) and including treatment (center of the circle untreated, outline treated with LPS). *C,* Macrophages from PC1 KO mice exhibit increased membrane targeted molecules involved in vesicle-associated functions. The number of membrane-targeted molecules, here defined as molecules with a membrane/cytoplasm ratio >2, was higher in macrophages derived from KO mice as compared with macrophages from WT mice. Genes coding for KO-specific membrane-targeted molecules were significantly enriched in genes annotated with GO terms describing vesicle-associated functions or cellular compartments. These included the GO term "extracellular vesicular exosome" (p = 1.75E-11) in unstimulated macrophages and the GO term "post-Golgi vesicle-mediated transport" (p = 0.009) in LPS-stimulated macrophages.

(Il1Rap), a known active factor in TLR4 signaling that functions by mediating IL-1-dependent activation of NF-κB in the MyD88-dependent pathway. Moreover, the cytoplasmic inhibitor of TLR4 signaling, NLRX1, was under-expressed in both resting and challenged PC1/3-K_D cells (49). Finally, we observed that molecules co-expressed with NF-κB1 in LPS-stimulated K_D cells comprised Stat1 and Stat2, two major pro-inflammatory transcription factors that were not co-expressed with NF-κB1 in LPS-stimulated NT cells (Fig. 7). To determine whether NF-κB showed greater activation in PC1/3-K_D cells, we conducted Western blot studies of the TLR4 signaling pathway by studying IκB-α phosphorylation and IRF3 nuclear translocation (Fig. 8).

The fold change represents the ratio of the band intensity between LPS-stimulated and nonstimulated samples at each time point. The kinetics of the phosphorylation of IκB-α after LPS challenge from 1 h to 6 h clearly showed that the fold change in phosphorylated IκB-α was higher at 3 h in K_D cells compared with NT cells (Fig. 8*A*a, a′ and 8*B*a). At 1 h, the phosphorylation of IκB-α was high in both NT and K_D cells. This phosphorylation remained high in K_D cells at 3 h, whereas it decreased in NT cells. In K_D cells, a decrease in IκB-α

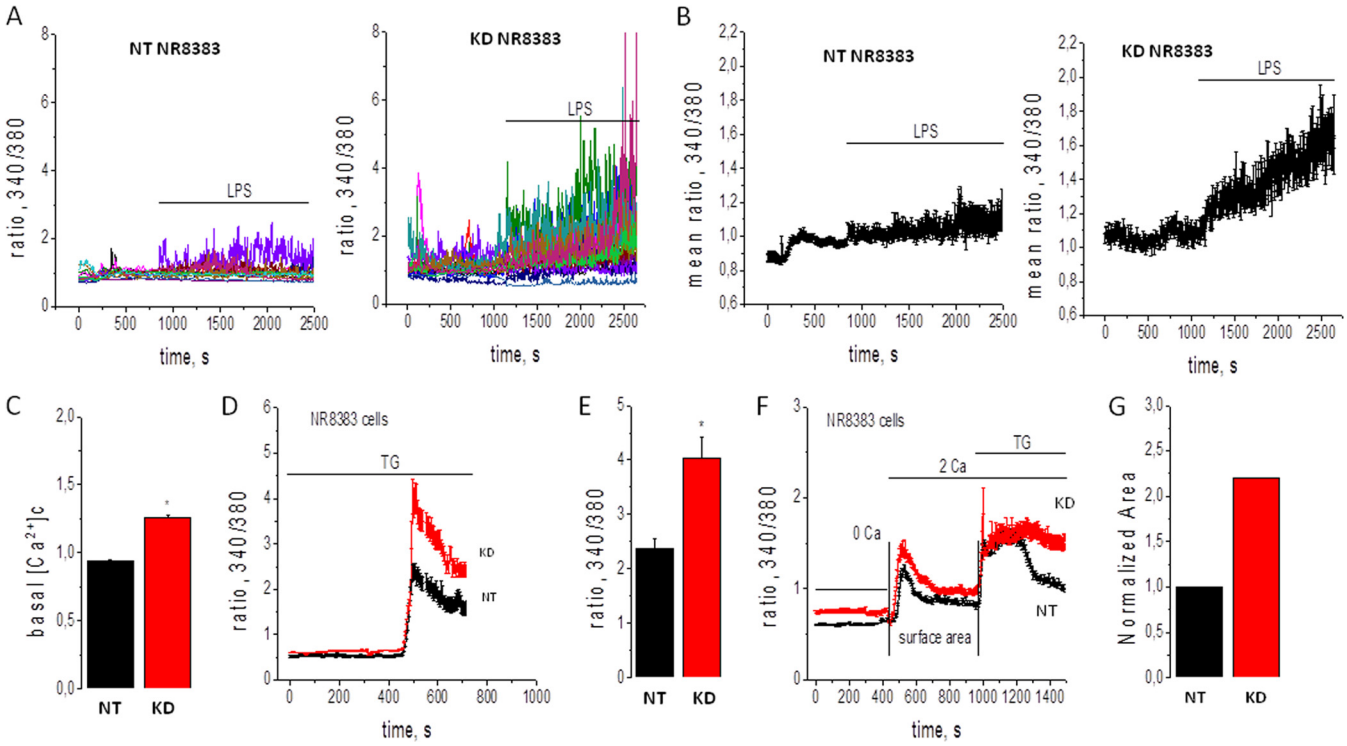

FIG. 6. **PC1/3-knockdown induces remodeling of Ca^{2+} homeostasis.** *A*, The cytosolic calcium concentration ((Ca^{2+})c) rose in NT and K_D NR8383 cells in response to LPS (horizontal bar). *B*, Quantification of the results presented in A. *C*, Quantification of the resting (Ca^{2+})c in NT and K_D NR8383 cells under basal conditions. *D*, Representative measurements of TG-activated SOCE, as indicated by the elevated (Ca^{2+})c in NR8383 cells. *E*, Quantification of SOCE in the results presented in *D*. *F*, The (Ca^{2+})c in the presence of 0 or 2 mM extracellular Ca^{2+} and after TG treatment in NT or K_D NR8383 cells. *G*, Quantification of the surface area presented in F following the application of 2 mM extracellular Ca^{2+}. $n = 3$.

TABLE V

List of selected identified proteins implicated in the immune system in NT and K_D PC1/3 resting (control) or LPS-stimulated macrophages

	Protein name	Gene name	NT		K_D	
			control	LPS	control	LPS
Chemokines and cytokines	Interleukin-1 receptor accessory protein	Il1rap	19.0246	19.2564	18.8126	20.2122
	C-X-C motif chemokine 2	Cxcl2	-	21.6242	-	22.83
	C-C motif chemokine 4	Ccl4	-	21.7711	21.7329	22.0981
	C-C motif chemokine 3	Ccl3	22.5974	27.755	24.8941	27.4812
	Macrophage migration inhibitory factor	Mif	28.5274	27.1267	26.8169	26.1873
Interferon-induced protein	Protein Ifit1	Ifit1	-	22.4039	-	24.6132
	Interferon-induced guanylate-binding protein 2	Gbp2	22.6232	24.1038	23.732	25.3116
TLR4 signaling	Nuclear factor NF-kappa-B p105 subunit	Nfkb1	19.4862	21.1055	21.2137	22.8011
	NF-kappa-B essential modulator	Ikbkg	20.5364	20.8487	20.5426	19.4019
	Interferon regulatory factor 3	Irf3	21.2062	20.5156	19.5384	19.2483
	Monocyte differentiation antigen CD14	Cd14	-	25.1175	-	18.7208
Other	Low affinity Fc-gamma receptor IIB isoform 1	Fcgr2b	26.4859	26.4101	20.9933	22.2522
	Interferon regulatory factor 5	Irf5	19.3744	19.9151	20.3435	20.7204

phosphorylation was observed at 6 h. These features demonstrate that in K_D cells, IκB-α phosphorylation was observed for a longer period, leading to NF-κB activation. The TLR4 MyD88-dependent pathway was involved at later stages compared with NT cells. We also focused on the TLR4 MyD88-independent pathway by examining the nuclear translocation of IRF3. After 3 h and 6 h of LPS stimulation, a duplication of the band corresponding to the various phosphorylated states of IRF3 was observed (Fig. 8*A*b′). However, no significant difference in IRF3 nuclear translocation was observed between NT and K_D cells over time (Fig. 8*B*b), suggesting that this pathway was not impacted by PC1/3 K_D (Fig. 8*A*b, b′ and 8*B*c). These data confirmed that NF-κB was mainly activated in PC1/3-K_D cells, as expected based on the proteomic analysis of the NR8383 cellular extracts. This phenomenon is also consistent with our results showing the remodeling of the endosomal compartment (10), (11) (Table IV) and perturbations in calcium homeostasis (Fig. 6).

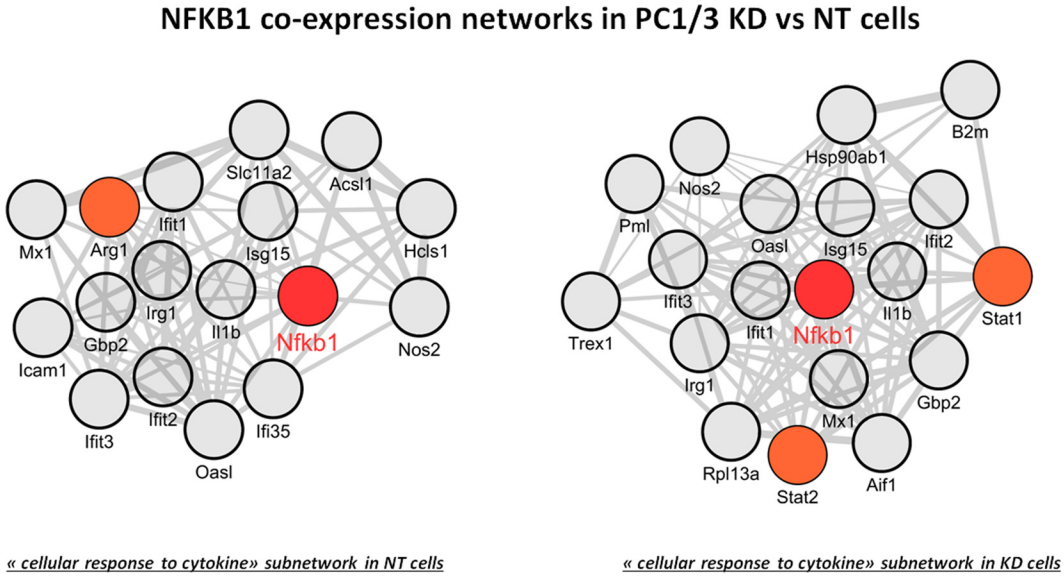

FIG. 7. **NFKB1 co-expression networks in PC1/3 K_D *versus* NT cells.** Lists of 100 genes which encoded molecules are the most tightly coregulated with NFKB1 in K_D or NT cells under LPS stimulation were established and assessed for gene set enrichment. Shown are subnetworks of genes annotated by the GO term "cellular response to cytokine stimuli" (adjusted p value for enrichment significance = 9.48e-6 in NT cells and 3.4e-7 in K_D cells). Note that Arg1, a prototypic M2 molecule, is specific to the NT subnetwork whereas Stat1 and Stat2, major pro-inflammatory transcription factors, are co-expressed with NFKB1 in K_D but not NT cells.

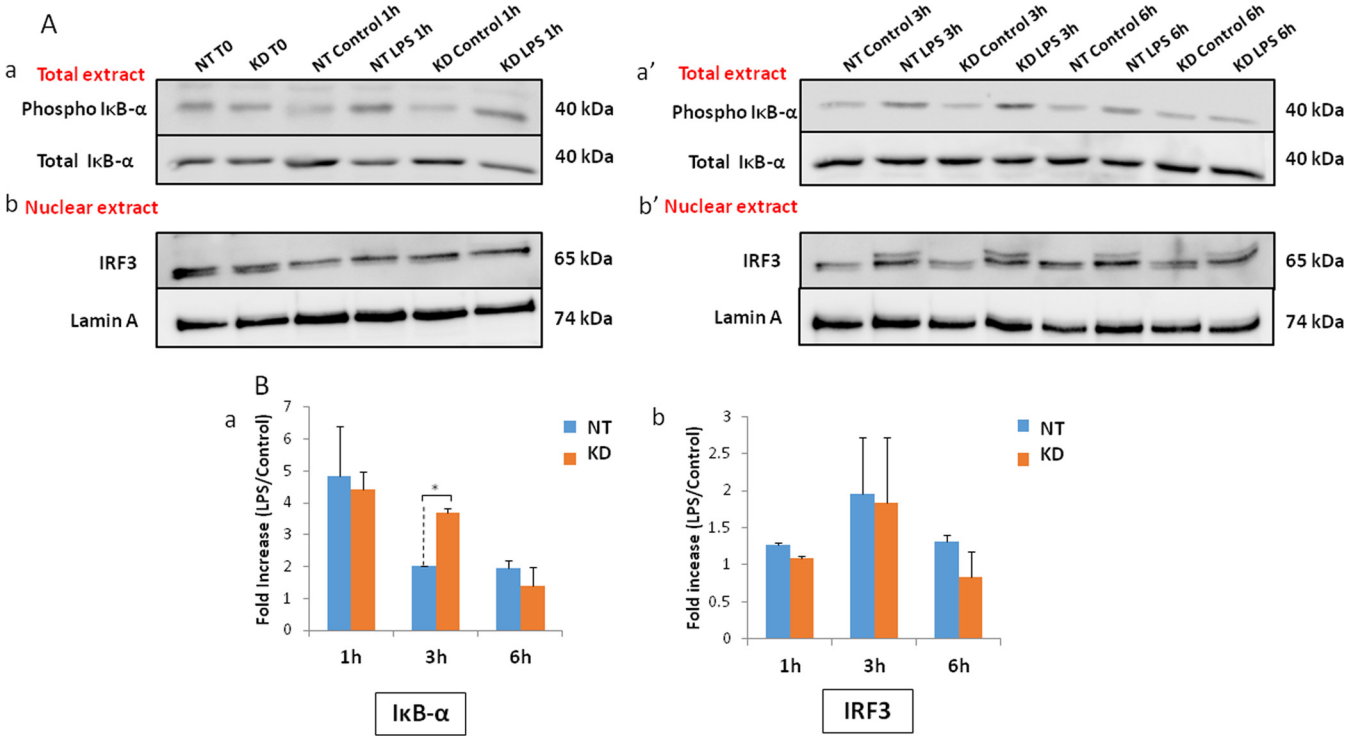

FIG. 8. **Western blot analysis of the TLR4 signaling pathway.** *A*, Western blot analysis of phospho IκB-α, total IκB-α (in total extracts, a and a'), IRF3 and Lamin A (in nuclear extracts, b and b') in NT or K_D PC1/3 NR8383 macrophages after LPS stimulation (200 ng/ml) or not at 1 h, 3 h and 6 h. *B*, Graphic representations of the quantification of phospho IκB-α (a) and IRF3 (b). The data are represented as the fold increase in samples stimulated with LPS relative to nonstimulated samples for phospho IκB-α and IRF3 and normalized to total IκB-α and Lamin A, respectively. * Significant differences between NT cells and K_D cells ($p \leq 0.05$) by t test. Experiments were performed in triplicate.

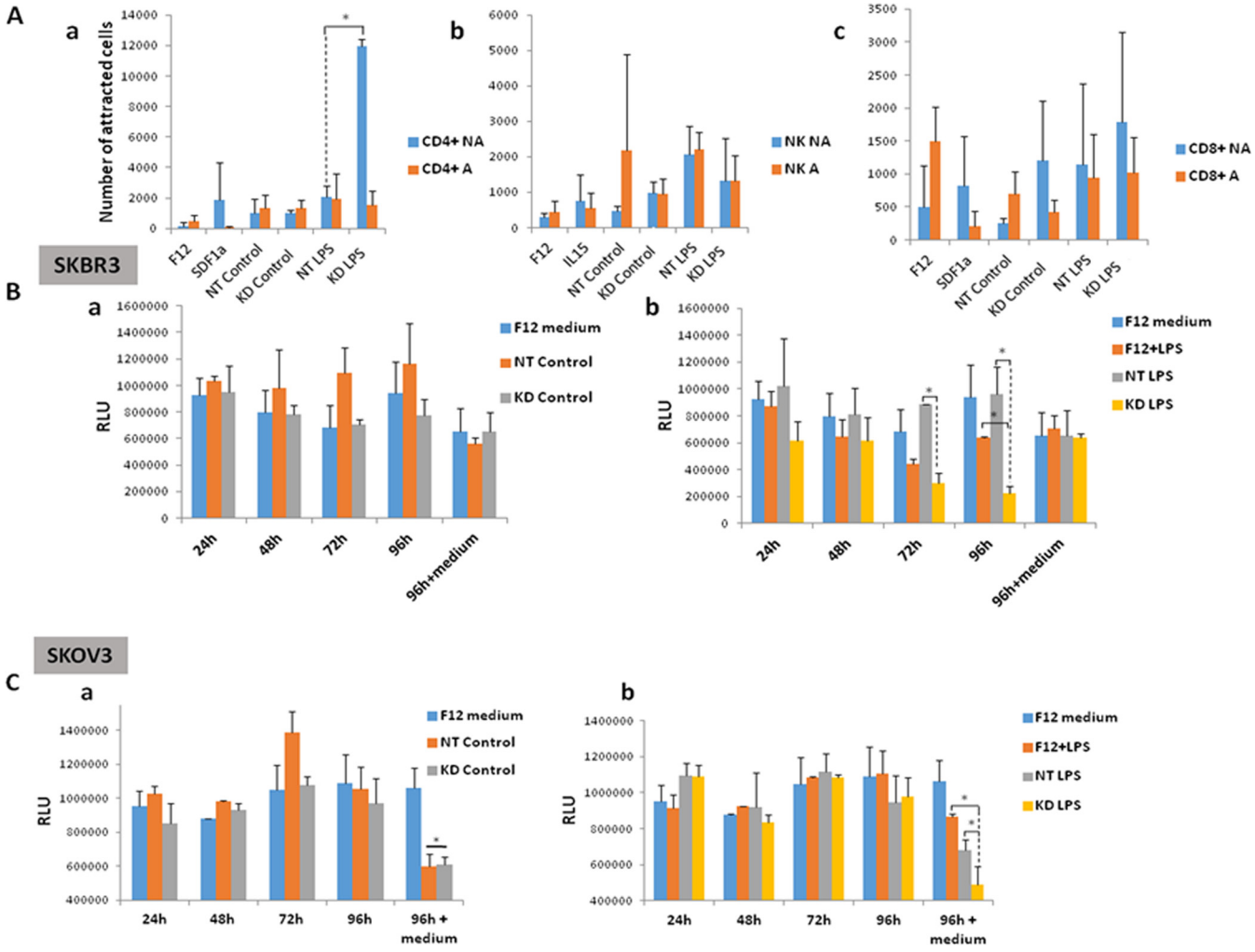

FIG. 9. **Chemoattraction and antitumor properties of NR8383 secretomes.** *A*, NR8383 PC1/3-K_D secretome enhanced CD4+ NA cell chemotaxis. Human primary leukocytes (CD4+ (a), natural killer (NK) cells (b) and CD8+ (c) cells that were activated (*A*) or nonactivated (NA)) were incubated in a Boyden chamber with NR8383 secretomes obtained at 24 h (control nonstimulated or stimulated with LPS) or F12 medium in the lower compartment. SDF1a and IL15 were used as controls for migration. Migration was conducted for 150 min. The results are presented as the number of cells that migrated. The experience was done in triplicates. *B*, *C*, The cell viability of SKBR3 cells (*B*) and SKOV3 cells (*C*) was determined using the CellTiter-Glo assay. The cells were incubated with NR8383 secretomes obtained at 24 h after no stimulation (a) or LPS stimulation (b). The assays were conducted for 24 h, 48 h, 72 h and 96 h. At 72 h, conditioned medium was replaced completely with fresh medium (96 h+ medium). The results were representative of three independent experiments. Significant differences were identified using Student's *t* test. $^*p < 0.05$.

Chemoattraction and Antitumor Activities of PC1/3-K_D Macrophage Secretomes—PC1/3 down-regulation in NR8383 macrophages strongly affected morphology and intracellular signaling pathways, leading to the secretion of large amounts of alarmins and pro-inflammatory chemokines and cytokines. These changes clearly suggest that PC1/3 K_D polarizes NR8383 toward an M1-like profile. M1 phenotype is characterized by high antigen presentation, high production of nitric oxide and high production of pro-inflammatory cytokines. They are known to have a killing function. In contract, M2 macrophages have repairing functions and produce high concentration of anti-inflammatory cytokines like IL-10.

The chemokines released by PC1/3-K_D macrophages are involved in leukocyte migration and activation (34) (Fig. 2*B*). CXCL10 (also known as IFN-γ-inducible protein of 10 kDa or IP-10) and CXCL9 (also known as monokine induced by IFN-γ or MIG) mainly function in T cell chemoattraction. These two chemokines share a common receptor: CXCR3. CXCR3 appears to be preferentially expressed on T lymphocytes (50). CCL20 is another chemokine that has been implicated in T cell chemoattraction, and the expression of its receptor, CCR6, has been detected in T and B lymphocytes (51). To investigate whether PC1/3-K_D NR8383 secretomes have chemotactic properties, assays were conducted in naïve (NA) or activated (A) T lymphocytes (CD4+, CD8+) and natural killer (NK) cells (Fig. 9*A*). Chemotaxis was performed in Boyden chambers using NR8383 secretomes as chemoattractant agents. The secretomes were obtained from

nonstimulated or LPS-stimulated NT or PC1/3-K_D macrophages after 24 h.

There was a significant attraction of CD4+ NA cells in the presence of the stimulated NR8383 PC1/3-K_D secretome (K_D LPS). We noticed a 6-fold increase in the attraction of CD4+ NA between NT LPS and K_D LPS secretomes (Fig. 9*A*a). No significant differences in chemoattraction were observed between NK and CD8+ cells (Figs. 9*A*b and c). The data indicated that immune factors produced by K_D cells following LPS challenge attracted naïve T helper lymphocytes (Th0; Fig. 9*A*a). Moreover, the nature of the chemokines and cytokines produced by the PC1/3-K_D cells could polarized these cells from a Th0 to a Th1 profile (TNF-α, IL-1α and IL-1β).

Next, we assessed the cytotoxic activities of NR8383 secretomes in the SKBR3 breast cancer cell line (Fig. 9*B*). The relative luminescence is proportional to cell viability and represents a measure of the level of ATP. Treatment with the supernatants of nonstimulated macrophages (control) did not affect the number of living cells (Fig. 9*B*a). Treatment with the supernatants of LPS-stimulated macrophages led to a decrease in the number of living cells at 72 h and 96 h (Fig. 9*B*b). A 3-fold decrease in the intensity of luminescence was observed between NT and K_D cell secretomes (LPS) at 72 h. At 96 h, a 5-fold decrease was observed. The decreased number of living SKBR3 cells demonstrated the anti-proliferative activity of PC1/3-K_D cell supernatants following LPS stimulation. Toxic tumor effects resulted from K_D macrophage activation and were mediated by soluble factors which is in line with the high level of chemokines secreted under LPS treatment. Moreover, LPS challenge triggers the release of specific factors impacting the viability of cancer cells. Such factors are absent in naive cells secretomes.

We then conducted these tests in an ovarian cancer cell line (SKOV3; Fig. 9*C*). The results confirmed that the secreted factors from PC1/3-K_D macrophages exerted antitumor activities, but in different ways, depending on the cell line considered. In SKOV3 cells, the effects were registered at 96 h after refreshing the conditioned medium with activated secreted factors from LPS-challenged PC1/3-K_D macrophages (Fig. 9*C*b). Under these conditions, NT and K_D cells in sterile conditions affected the viability of the SKOV3 tumor cells. A 1.7-fold decrease in luminescence intensity was observed when the cells were exposed to nonstimulated NT and K_D cell secretomes (Fig. 9*C*a). In LPS-challenged conditions, this decrease was 2.2 fold for the K_D secretome and 1.4-fold for the NT secretome.

These results suggested that these two cell lines did not have the same sensitivity toward factors secreted by PC1/3-K_D macrophages. SKBR3 cells were more sensitive to the direct actions of the secreted factors. SKOV3 cells were sensitized by these factors, and renewal of the conditioned medium with fresh medium containing the same secreted proteins affected their proliferation. This difference in response to treatment between SKBR3 and SKOV3 cells was noted recently (52). One major difference between these two cell lines is the production of inhibitory cytokines, such as IL-10: SKBR3 cells produce IL-10, whereas SKOV3 cells do not. Nevertheless, in both cases, the factors secreted by PC1/3-K_D NR8383 cells were active toward the tumor cells. In those conditions, we assessed whether PC1/3-K_D cells were susceptible to IL-10 in terms of their secretion of pro-inflammatory cytokines. As observed in Fig. 10, in response to Il-10 treatment, NT and K_D cells secreted decreased amounts of the pro-inflammatory chemokines CXCL1, CXCL2, TNF-α, and IL1–10. However, K_D cells were more resistant to this inhibition and could be more resistant to the tumor inhibitory medium. After IL-10 inhibition, cells were then challenged with LPS. In that case chemokine secretion was restored in both NT and K_D cells. Of note, a significant increase in chemokine release was again observed in K_D cells, especially for CXCL1, CXCL2, CXCL10, IL1-α, and IL-6. These results clearly demonstrate that PC1/3 K_D cells still conserve their M1-like phenotype under inhibitory conditions and that the immune profile is pro-inflammatory.

DISCUSSION

The data from our current work demonstrate that PC1/3 is a key enzyme involved in the regulation of cytokine secretion and, consequently, is important for the regulation of macrophage activation, as depicted in Fig. 11.

When PC1/3 was inhibited, immune factors such as pro-inflammatory chemokines as well as alarmins (GRP78, HSP84, HSP86, HSP73, calreticulin, capthepsin B, nucleolin, granulins) were secreted in the absence of challenge. These alarmins may act as autocrine and paracrine factors and activate an immune response through TLR4 (53). Immune factors, such as IL-6 and TNF-α, are known to be produced by immune cells through the canonical ER-Golgi secretion pathway. However, in NR8383-K_D macrophages, numerous unconventional vesicular or organellar pathways have been found. Indeed, proteomic analyses of cell extracts have revealed that the canonical secretion pathway is deregulated and the noncanonical secretion machinery, with an accumulation of endosomes and MVBs, is reinforced. A large number of studies have shown that many proteins known to regulate endocytosis also participate in nuclear signaling. Among them, an adaptor protein containing a pleckstrin homology domain, a phosphotyrosine binding domain and leucine zipper motif 1 (APPL1) has a role in the positive regulation of NF-κB signaling. The overexpression of APPL1 triggers p65 translocation to the nucleus in the absence of stimulation (54). Annexin A6 has been shown to increase NF-κB activity in response to activation signals (55). These two proteins are over-expressed in PC1/3-K_D macrophages and may have an impact on TLR4 signaling (Table IV). Co-expression networks analysis showed that two major pro-inflammatory transcription factors, Stat1 and Stat2, are co-expressed with NF-κB1 in PC1/3-K_D cells whereas Arg1, a prototypic M2 molecule, is

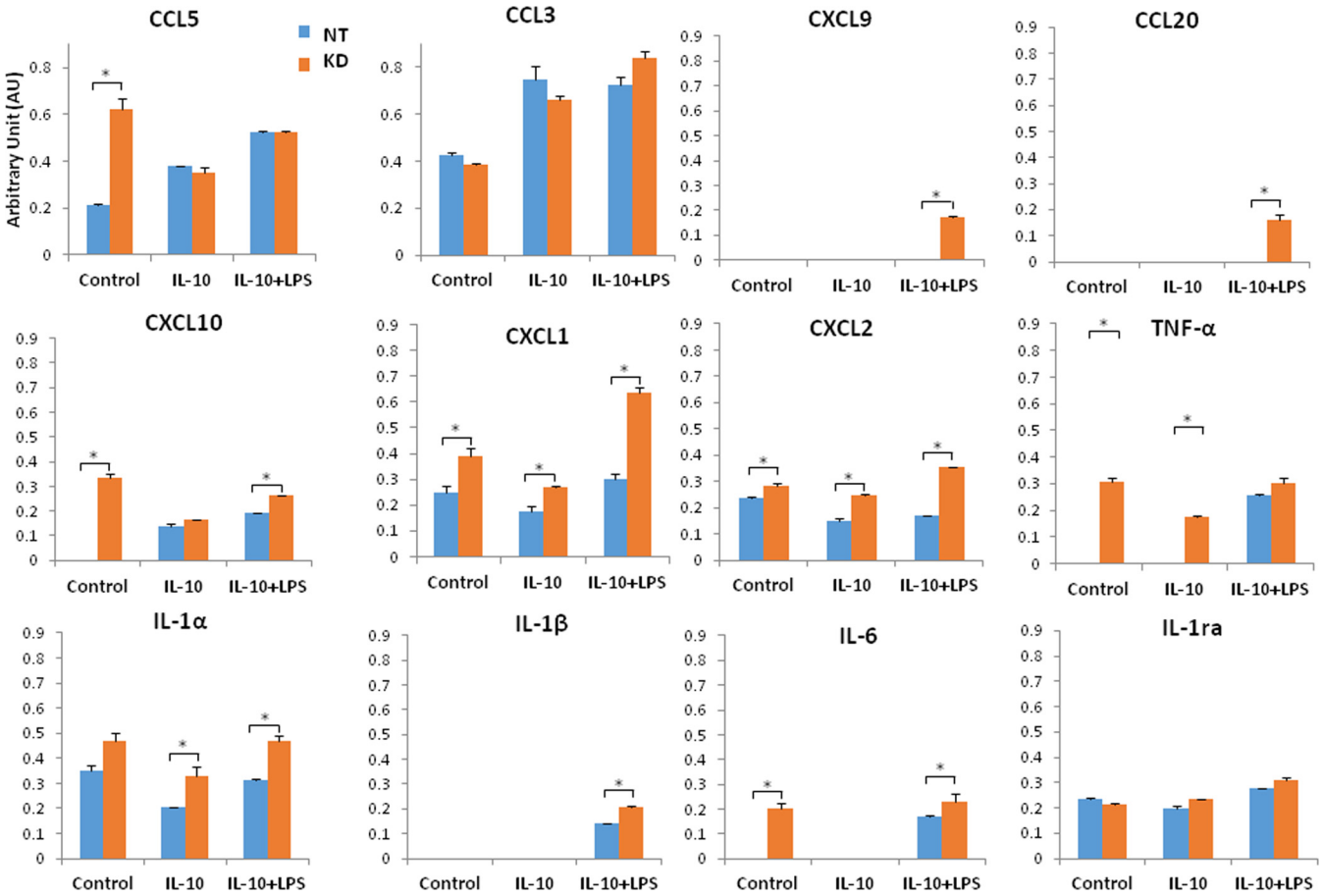

FIG. 10. **Effect of PC1/3 down-regulation on cytokine secretion under inhibitory conditions.** The rat cytokine array assay was performed in NR8383 secretomes (NT/K_D). The cells were untreated (control) or treated with IL-10 for 24 h without stimulation (IL-10) or with LPS for 24 h (IL-10+LPS). Blue shows NT cell secretomes, and orange indicates K_D cell secretomes. The bar diagrams represent the ratio of the spot mean pixel densities/reference point pixel densities. Significant differences were analyzed using Student's *t* test. *$p < 0.05$.

specific to the NT subnetwork (Fig. 7). Proteomics and Western blot analysis revealed that in PC1/3-K_D cells, the MyD88-dependent pathway was sustained. As a result, a greater activation of NF-κB was observed. This transcription factor is known to regulate the expression of the pore-forming Ca^{2+} channel unit, Orai1, and its activator, STIM1, to control Ca^{2+} entry and affect cellular functions (56). The induction of NF-κB by ER stress, *i.e.* Ca^{2+} efflux from the ER, has been also observed (57), and this induction is inhibited by Ca^{2+} chelators (58). Moreover, the treatment of cells with thapsigargin, which causes an efflux of Ca^{2+} from the ER, leads to NF-κB translocation (58). In the present study, we showed that, in PC1/3-K_D cells, both basal Ca^{2+} and constitutive Ca^{2+} influx increased. This result is consistent with our findings about NF-κB activation (Figs. 7 and 8). Calcium is also known to interact with cytoskeletal proteins. In PC1/3-K_D cells, cytoskeletal proteins were over-expressed, leading to the formation of a large number of filopodia (Figs. 3 and 4). The cell elasticity determines macrophage functions and is known to regulate phagocytosis or LPS responsiveness. In a positive feedback loop, the cytoskeleton can modulate the intracellular trafficking machinery through microtubules and calcium mobilization (59, 60). This event may amplify such a phenomenon and explain the spontaneous release of pro-inflammatory cytokines. In response to LPS challenge, amplified effects were registered in these PC1/3-K_D cells, provoking increased Ca^{2+} entry and thus impacting the morphology of the cells by producing a greater number of filopodia. As a result, these cells secreted more chemokines and cytokines to recruit naïve T helper lymphocytes (CD4+) and to orient the immune response from Th0 to Th1. Altogether, these findings show that PC1/3-K_D macrophages exhibit an M1-like phenotype.

It is known that, during the tumor development process, M1-polarized macrophages switch to an M2-like phenotype that is characterized by IL-12^{low} IL-10^{high} and lose their tumoricidal activities (61). According to our results, PC1/3 inhibition could be a relevant strategy to reverse the macrophage phenotype from an M2-like to an M1-like phenotype. As a first step, we tested whether the inhibitory cytokine IL-10 could

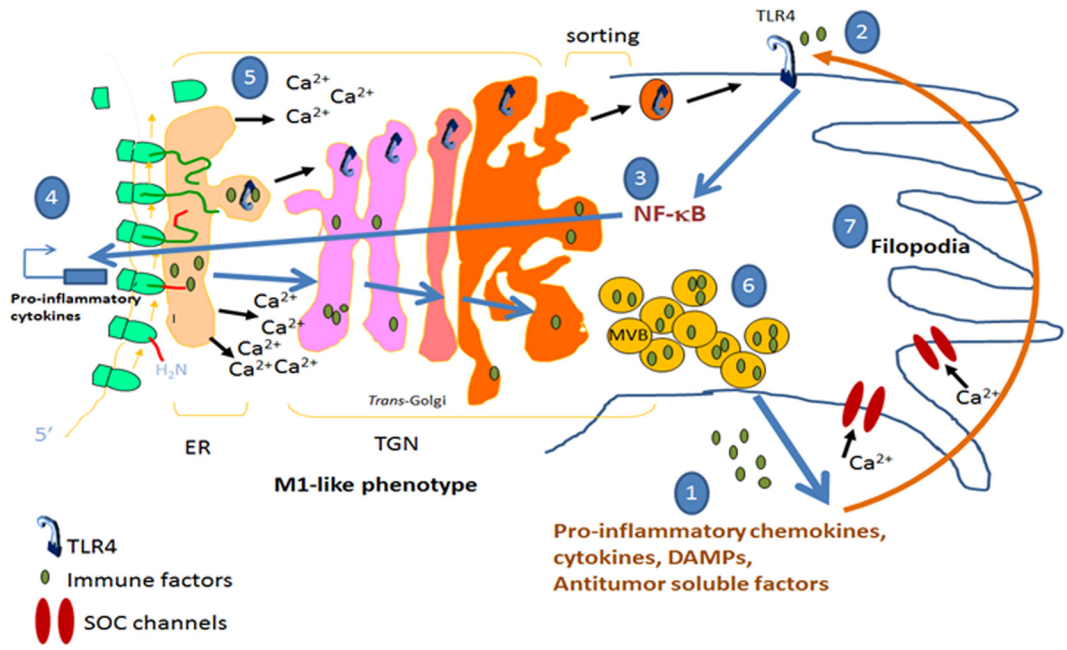

FIG. 11. **Schematic depicting how PC1/3 knockdown impacts macrophage activation based on the data presented in Figs. 1–8.** PC1/3 knockdown promotes the formation of endosomes and MVB release of inflammatory chemokines and cytokines via the noncanonical secretion pathway (1). Danger signal molecules (DAMs) can activate TLR4 (2) and induce the MyD88-dependent pathway with increased NF-κB (3) nuclear translocation (4) linked to Ca^{2+} mobilization in PC1/3 K_D macrophages (5). Both of these phenomena are also implicated in cytokines, chemokines, DAMs and tumor viability inhibitor release (6) as well as cytoskeletal rearrangements leading to the formation of filopodia (7). We then noticed that during LPS challenge, the amplification loop was amplified and driven toward the induction of increased Ca^{2+} release from the ER, greater numbers of filopodia and MVBs, the release of additional immune factors, an M1 phenotype refractive to IL-10 inhibition and a greater number of anti-tumor factors.

affect the secretion properties of PC1/3-K_D macrophages. Despite IL-10 treatment, these cells still spontaneously released pro-inflammatory cytokines and oriented the immune response toward a cytotoxic one. Thus, these cells clearly remained highly active. Moreover, in response to LPS challenge, their level of reactivity was restored to the same level of significance as that in cells challenged with LPS without IL-10. We also confirmed the antitumoral properties of their secretomes toward two different cell lines, *i.e.* one that is known to produce large amounts of IL-10 (SKBR3), whereas the other does not (SKOV3). Taken together, we demonstrated that PC1/3 K_D affected cell viability and resistance of cancer cells by the more abundant release of antitumoricidal factors such as TNF-α (62). PC1/3 is thus a promising target to reactivate dormant immune cells in tumors and in immunotherapeutic strategies.

Acknowledgments—We thank Elodie Richard of the CCMIC-Université de Lille 1 (BiCel) for her help and technical support in confocal microscopy experiments.

* This work was funded by grants from the Ministère de L'Education Nationale, de L'Enseignement Supérieur et de la Recherche, ANR (IF), Région Nord-Pas de Calais ARCIR (IF), the Université de Lille (MD) SIRIC ONCOLille (IF, MD), Grant INCa-DGOS-Inserm 6041aa, the CCMIC and INSERM.

S This article contains supplemental Data S1 to S6.

¶¶ To whom correspondence should be addressed: U-1192 Inserm, Laboratoire de Protéomique, Réponse Inflammatoire, Spectrométrie de Masse (PRISM), Université de Lille 1, Cité Scientifique, 59655 Villeneuve D'Ascq, France. Tel.: +33 (0)3 20 43 41 94; Fax: +33 (0)3 20 43 40 54; E-mail: michel.salzet@univ-lille1.fr.

Competing financial interests: The authors declare no competing financial interests.

REFERENCES

1. Ward, A. E., and Rosenthal, B. M. (2014) Evolutionary responses of innate immunity to adaptive immunity. *Infection, Genetics Evolution* **21,** 492–496
2. Buchmann, K. (2014) Evolution of Innate Immunity: Clues from Invertebrates via Fish to Mammals. *Front. Immunol.* **5,** 459
3. Wang, N., Liang, H., and Zen, K. (2014) Molecular mechanisms that influence the macrophage m1-m2 polarization balance. *Front. Immunol.* **5,** 614
4. Takeda, K., and Akira, S. (2004) TLR signaling pathways. *Sem. Immunol.* **16,** 3–9
5. Ostuni, R., Kratochvill, F., Murray, P. J., and Natoli, G. (2015) Macrophages and cancer: from mechanisms to therapeutic implications. *Trends Immunol* **36,** 229–239
6. Salzet, M., and Day, R. (2003) [Endocrine markers of cellular immunity: defining the endocrine phenotype). *J. Soc. Biol.* **197,** 97–101
7. Salzet, M. (2002) Immune cells express endocrine markers. *Neuro. Endocrinol. Lett.* **23,** 8–9
8. Salzet, M., Vieau, D., and Day, R. (2000) Crosstalk between nervous and immune systems through the animal kingdom: focus on opioids. *Trends Neurosci.* **23,** 550–555
9. Brogden, K. A., Guthmiller, J. M., Salzet, M., and Zasloff, M. (2005) The nervous system and innate immunity: the neuropeptide connection. *Nat. Immunol.* **6,** 558–564
10. Refaie, S., Gagnon, S., Gagnon, H., Desjardins, R., D'Anjou, F., D'Orléans-Juste, P., Zhu, X., Steiner, D. F., Seidah, N. G., and Lazure, C. (2012)

Disruption of Proprotein Convertase 1/3 (PC1/3) Expression in Mice Causes Innate Immune Defects and Uncontrolled Cytokine Secretion. *J. Biol. Chem.* **287,** 14703–14717
11. Gagnon, H., Refaie, S., Gagnon, S., Desjardins, R., Salzet, M., and Day, R. (2013) Proprotein convertase 1/3 (PC1/3) in the rat alveolar macrophage cell line NR8383: localization, trafficking and effects on cytokine secretion. *PLoS ONE* **8,** e61557
12. Lansac, G., Dong, W., Dubois, C. M., Benlarbi, N., Afonso, C., Fournier, I., Salzet, M., and Day, R. (2006) Lipopolysaccharide mediated regulation of neuroendocrine associated proprotein convertases and neuropeptide precursor processing in the rat spleen. *J. Neuroimmunol.* **171,** 57–71
13. Refaie, S., Gagnon, S., Gagnon, H., Desjardins, R., D'Anjou, F., D'Orleans-Juste, P., Zhu, X., Steiner, D. F., Seidah, N. G., Lazure, C., Salzet, M., and Day, R. (2012) Disruption of proprotein convertase 1/3 (PC1/3) expression in mice causes innate immune defects and uncontrolled cytokine secretion. *J. Biol. Chem.* **287,** 14703–14717
14. Wisniewski, J. R., Ostasiewicz, P., and Mann, M. (2011) High recovery FASP applied to the proteomic analysis of microdissected formalin fixed paraffin embedded cancer tissues retrieves known colon cancer markers. *J. Proteome Res.* **10,** 3040–3049
15. Meissner, F., Scheltema, R. A., Mollenkopf, H. J., and Mann, M. (2013) Direct proteomic quantification of the secretome of activated immune cells. *Science* **340,** 475–478
16. Polati, R., Castagna, A., Bossi, A., Campostrini, N., Zaninotto, F., Timperio, A. M., Zolla, L., Olivieri, O., Corrocher, R., and Girelli, D. (2009) High resolution preparation of monocyte-derived macrophages (MDM) protein fractions for clinical proteomics. *Proteome Sci.* **7,** 4
17. Searle, B. C. (2010) Scaffold: a bioinformatic tool for validating MS/MS-based proteomic studies. *Proteomics* **10,** 1265–1269
18. Shilov, I. V., Seymour, S. L., Patel, A. A., Loboda, A., Tang, W. H., Keating, S. P., Hunter, C. L., Nuwaysir, L. M., and Schaeffer, D. A. (2007) The Paragon Algorithm, a next generation search engine that uses sequence temperature values and feature probabilities to identify peptides from tandem mass spectra. *Mol. Cell. Proteomics* **6,** 1638–1655
19. Tang, W. H., Shilov, I. V., and Seymour, S. L. (2008) Nonlinear fitting method for determining local false discovery rates from decoy database searches. *J. Proteome Res.* **7,** 3661–3667
20. Colinge, J., Chiappe, D., Lagache, S., Moniatte, M., and Bougueleret, L. (2005) Differential proteomics via probabilistic peptide identification scores. *Anal. Chem.* **77,** 596–606
21. Gotz, S., Garcia-Gomez, J. M., Terol, J., Williams, T. D., Nagaraj, S. H., Nueda, M. J., Robles, M., Talon, M., Dopazo, J., and Conesa, A. (2008) High-throughput functional annotation and data mining with the Blast2GO suite. *Nucleic Acids Res.* **36,** 3420–3435
22. Szklarczyk, D., Franceschini, A., Kuhn, M., Simonovic, M., Roth, A., Minguez, P., Doerks, T., Stark, M., Muller, J., Bork, P., Jensen, L. J., and von Mering, C. (2011) The STRING database in 2011: functional interaction networks of proteins, globally integrated and scored. *Nucleic Acids Res.* **39,** D561–568
23. Smoot, M. E., Ono, K., Ruscheinski, J., Wang, P. L., and Ideker, T. (2011) Cytoscape 2.8: new features for data integration and network visualization. *Bioinformatics* **27,** 431–432
24. Saito, R., Smoot, M. E., Ono, K., Ruscheinski, J., Wang, P. L., Lotia, S., Pico, A. R., Bader, G. D., and Ideker, T. (2012) A travel guide to Cytoscape plugins. *Nat. Methods* **9,** 1069–1076
25. Cox, J., and Mann, M. (2008) MaxQuant enables high peptide identification rates, individualized p.p.b.-range mass accuracies and proteome-wide protein quantification. *Nat. Biotechnol.* **26,** 1367–1372
26. Cox, J., Neuhauser, N., Michalski, A., Scheltema, R. A., Olsen, J. V., and Mann, M. (2011) Andromeda: a peptide search engine integrated into the MaxQuant environment. *J. Proteome Res.* **10,** 1794–1805
27. Cox, J., Hein, M. Y., Luber, C. A., Paron, I., Nagaraj, N., and Mann, M. (2014) Accurate proteome-wide label-free quantification by delayed normalization and maximal peptide ratio extraction, termed MaxLFQ. *Mol. Cell. Proteomics* **13,** 2513–2526
28. Vizcaino, J. A., Deutsch, E. W., Wang, R., Csordas, A., Reisinger, F., Rios, D., Dianes, J. A., Sun, Z., Farrah, T., Bandeira, N., Binz, P. A., Xenarios, I., Eisenacher, M., Mayer, G., Gatto, L., Campos, A., Chalkley, R. J., Kraus, H. J., Albar, J. P., Martinez-Bartolome, S., Apweiler, R., Omenn, G. S., Martens, L., Jones, A. R., and Hermjakob, H. (2014) ProteomeXchange provides globally coordinated proteomics data submission and dissemination. *Nat. Biotechnol.* **32,** 223–226
29. Vizcaino, J. A., Cote, R. G., Csordas, A., Dianes, J. A., Fabregat, A., Foster, J. M., Griss, J., Alpi, E., Birim, M., Contell, J., O'Kelly, G., Schoenegger, A., Ovelleiro, D., Perez-Riverol, Y., Reisinger, F., Rios, D., Wang, R., and Hermjakob, H. (2013) The PRoteomics IDEntifications (PRIDE) database and associated tools: status in 2013. *Nucleic Acids Res.* **41,** D1063–1069
30. Montojo, J., Zuberi, K., Rodriguez, H., Kazi, F., Wright, G., Donaldson, S. L., Morris, Q., and Bader, G. D. (2010) GeneMANIA Cytoscape plugin: fast gene function predictions on the desktop. *Bioinformatics* **26,** 2927–2928
31. Chen, E. Y., Tan, C. M., Kou, Y., Duan, Q., Wang, Z., Meirelles, G. V., Clark, N. R., and Ma'ayan, A. (2013) Enrichr: interactive and collaborative HTML5 gene list enrichment analysis tool. *BMC Bioinformatics* **14,** 128
32. Azzaoui, I., Yahia, S. A., Chang, Y., Vorng, H., Morales, O., Fan, Y., Delhem, N., Ple, C., Tonnel, A. B., Wallaert, B., and Tsicopoulos, A. (2011) CCL18 differentiates dendritic cells in tolerogenic cells able to prime regulatory T cells in healthy subjects. *Blood* **118,** 3549–3558
33. Bianchi, M. E. (2007) DAMPs, PAMPs and alarmins: all we need to know about danger. *J. Leukoc. Biol.* **81,** 1–5
34. Franciszkiewicz, K., Boissonnas, A., Boutet, M., Combadiere, C., and Mami-Chouaib, F. (2012) Role of chemokines and chemokine receptors in shaping the effector phase of the antitumor immune response. *Cancer Res.* **72,** 6325–6332
35. Duitman, E. H., Orinska, Z., Bulanova, E., Paus, R., and Bulfone-Paus, S. (2008) How a cytokine is chaperoned through the secretory pathway by complexing with its own receptor: lessons from interleukin-15 (IL-15)/IL-15 receptor alpha. *Mol. Cell. Biol.* **28,** 4851–4861
36. Takenawa, T., and Suetsugu, S. (2007) The WASP-WAVE protein network: connecting the membrane to the cytoskeleton. *Nat. Rev. Mol. Cell Biol.* **8,** 37–48
37. Patel, N. R., Bole, M., Chen, C., Hardin, C. C., Kho, A. T., Mih, J., Deng, L., Butler, J., Tschumperlin, D., Fredberg, J. J., Krishnan, R., and Koziel, H. (2012) Cell elasticity determines macrophage function. *PLoS ONE* **7,** e41024
38. Bonnemaison, M. L., Eipper, B. A., and Mains, R. E. (2013) Role of adaptor proteins in secretory granule biogenesis and maturation. *Front. Endocrinol.* **4,** 101
39. Chaineau, M., Danglot, L., Proux-Gillardeaux, V., and Galli, T. (2008) Role of HRB in clathrin-dependent endocytosis. *J. Biol. Chem.* **283,** 34365–34373
40. Hutagalung, A. H., and Novick, P. J. (2011) Role of Rab GTPases in membrane traffic and cell physiology. *Physiol. Rev.* **91,** 119–149
41. Savina, A., Furlan, M., Vidal, M., and Colombo, M. I. (2003) Exosome release is regulated by a calcium-dependent mechanism in K562 cells. *J. Biol. Chem.* **278,** 20083–20090
42. Valitutti, S., Dessing, M., Aktories, K., Gallati, H., and Lanzavecchia, A. (1995) Sustained signaling leading to T cell activation results from prolonged T cell receptor occupancy. Role of T cell actin cytoskeleton. *J. Exp. Med.* **181,** 577–584
43. Nolz, J. C., Gomez, T. S., Zhu, P., Li, S., Medeiros, R. B., Shimizu, Y., Burkhardt, J. K., Freedman, B. D., and Billadeau, D. D. (2006) The WAVE2 complex regulates actin cytoskeletal reorganization and CRAC-mediated calcium entry during T cell activation. *Curr. Biol.* **16,** 24–34
44. Sun, H. Q., Yamamoto, M., Mejillano, M., and Yin, H. L. (1999) Gelsolin, a multifunctional actin regulatory protein. *J. Biol. Chem.* **274,** 33179–33182
45. Panther, E., Durk, T., Ferrari, D., Di Virgilio, F., Grimm, M., Sorichter, S., Cicko, S., Herouy, Y., Norgauer, J., Idzko, M., and Muller, T. (2012) AMP affects intracellular Ca2+ signaling, migration, cytokine secretion and T cell priming capacity of dendritic cells. *PLoS ONE* **7,** e37560
46. Heo, D. K., Lim, H. M., Nam, J. H., Lee, M. G., and Kim, J. Y. (2015) Regulation of phagocytosis and cytokine secretion by store-operated calcium entry in primary isolated murine microglia. *Cell Signal.* **27,** 177–186
47. Smyth, J. T., Hwang, S. Y., Tomita, T., DeHaven, W. I., Mercer, J. C., and Putney, J. W. (2010) Activation and regulation of store-operated calcium entry. *J. Cell. Mol. Med.* **14,** 2337–2349
48. Lytton, J., Westlin, M., and Hanley, M. R. (1991) Thapsigargin inhibits the sarcoplasmic or endoplasmic reticulum Ca-ATPase family of calcium pumps. *J. Biol. Chem.* **266,** 17067–17071
49. Xia, X., Cui, J., Wang, H. Y., Zhu, L., Matsueda, S., Wang, Q., Yang, X., Hong, J., Songyang, Z., Chen, Z. J., and Wang, R. F. (2011) NLRX1

negatively regulates TLR-induced NF-kappaB signaling by targeting TRAF6 and IKK. *Immunity* **34,** 843–853
50. Farber, J. M. (1997) Mig and IP-10: CXC chemokines that target lymphocytes. *J. Leukoc. Biol.* **61,** 246–257
51. Krzysiek, R., Lefevre, E. A., Bernard, J., Foussat, A., Galanaud, P., Louache, F., and Richard, Y. (2000) Regulation of CCR6 chemokine receptor expression and responsiveness to macrophage inflammatory protein-3alpha/CCL20 in human B cells. *Blood* **96,** 2338–2345
52. Bjorkelund, H., Gedda, L., and Andersson, K. (2011) Comparing the epidermal growth factor interaction with four different cell lines: intriguing effects imply strong dependency of cellular context. *PLoS ONE* **6,** e16536
53. Lee, K. H., Jeong, J., and Yoo, C. G. (2013) Positive feedback regulation of heat shock protein 70 (Hsp70) is mediated through Toll-like receptor 4-PI3K/Akt-glycogen synthase kinase-3beta pathway. *Exp. Cell Res.* **319,** 88–95
54. Hupalowska, A., Pyrzynska, B., and Miaczynska, M. (2012) APPL1 regulates basal NF-kappaB activity by stabilizing NIK. *J. Cell Sci.* **125,** 4090–4102
55. Campbell, K. A., Minashima, T., Zhang, Y., Hadley, S., Lee, Y. J., Giovinazzo, J., Quirno, M., and Kirsch, T. (2013) Annexin A6 interacts with p65 and stimulates NF-kappaB activity and catabolic events in articular chondrocytes. *Arthritis Rheum.* **65,** 3120–3129
56. Eylenstein, A., Schmidt, S., Gu, S., Yang, W., Schmid, E., Schmidt, E. M., Alesutan, I., Szteyn, K., Regel, I., Shumilina, E., and Lang, F. (2012) Transcription factor NF-kappaB regulates expression of pore-forming Ca2+ channel unit, Orai1, and its activator, STIM1, to control Ca2+ entry and affect cellular functions. *J. Biol. Chem.* **287,** 2719–2730
57. Prell, T., Lautenschlager, J., Weidemann, L., Ruhmer, J., Witte, O. W., and Grosskreutz, J. (2014) Endoplasmic reticulum stress is accompanied by activation of NF-kappaB in amyotrophic lateral sclerosis. *J. Neuroimmunol.* **270,** 29–36
58. Pahl, H. L., Sester, M., Burgert, H. G., and Baeuerle, P. A. (1996) Activation of transcription factor NF-kappaB by the adenovirus E3/19K protein requires its ER retention. *J. Cell Biol.* **132,** 511–522
59. Joseph, N., Reicher, B., and Barda-Saad, M. (2014) The calcium feedback loop and T cell activation: how cytoskeleton networks control intracellular calcium flux. *Biochim. Biophys. Acta* **1838,** 557–568
60. Murtazina, D. A., Chung, D., Ulloa, A., Bryan, E., Galan, H. L., and Sanborn, B. M. (2011) TRPC1, STIM1, and ORAI influence signal-regulated intracellular and endoplasmic reticulum calcium dynamics in human myometrial cells. *Biol. Reprod.* **85,** 315–326
61. Chanmee, T., Ontong, P., Konno, K., and Itano, N. (2014) Tumor-associated macrophages as major players in the tumor microenvironment. *Cancers* **6,** 1670–1690
62. Wallach, D., and Kovalenko, A. (2009) 12th international TNF conference: the good, the bad and the scientists. *Cytokine Growth Factor Rev.* **20,** 259–269